10 Antifoaming and defoaming

> Fed officials used to think there was little they could do to prevent bubbles from inflating. Their strategy was to mop up after a bubble burst with lower interest rates.
>
> *Jon Hilsenrath, Wall Street Journal, 2 Dec, 2009.*

10.1 Background and types of antifoamers and defoamers

Although foams are thermodynamically unstable, under practical conditions they can remain fairly stable for a considerable period of time, and it is often necessary to add chemicals to prevent foaming or to destroy the foam. Early definitions of antifoamers referred to the chemicals or materials pre-dispersed in the liquid phase prior to processing to prevent foam formation (produce low foamability) while defoamers were added to eliminate existing stable foams (produce low foam stability) by a shock effect. However, today this distinction is confusing since most chemical additives cover several roles and the nomenclature varies according to the industry where they are used. In fact, they are often referred to as foam control agents, foam inhibitors, foam suppressants and air release agents.

Foaming causes problems throughout a range of industrial processes, for example, in the production and processing of paper, pharmaceuticals, materials, textiles, coatings, crude oil, washing, leather, paints, adhesives, lubrication, fuels, heat transfer fluids and so on. In the processing of food and beverages such as sugar beet, orange and tomato juice, beer, wine and mashed potatoes, foaming problems caused by soluble proteins and starch are commonly encountered. Food containers are washed and recycled and again foaming must be prevented during these processes. It is also frequently necessary to break foam in storage vessels to increase the capacity (such as beer), and foam breaking is necessary to increase the efficiency of distillation or evaporation processes. There are numerous reviews of the antifoaming/defoaming area and a comprehensive book by Garrett (1) in 1993 covers the basic physical chemistry and most of the industrial uses of antifoamers. A more recent publication by Garrett (2) in 2015 summarizes further developments associated with the mode of action and also the mechanical aspects of defoaming are reviewed. Early publications by Owen (3) classify different products, and Kerner (4) lists the antifoaming products supplied by major companies. There are over 100 suppliers, if smaller companies are included, and many international suppliers have

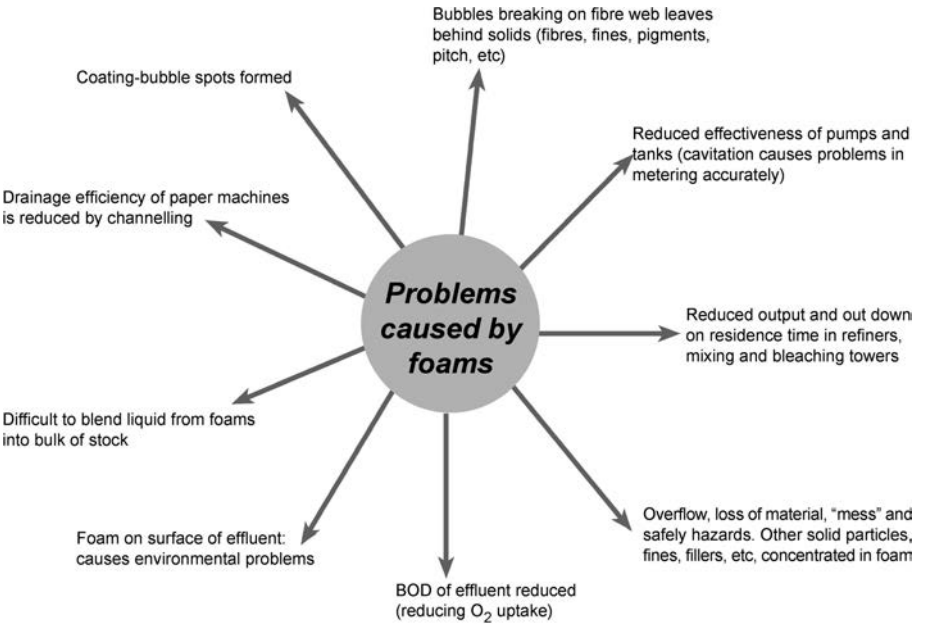

Fig. 10.1 Problems caused by foams in the pulp and paper industry. From ref (5).

manufacturing capacity whereas smaller companies specialize in formulations for particular industries or processes.

The most important usage of antifoamers is in the pulp and paper industry, where voluminous and stable foams frequently appear at various stages in the processing. These are caused by the release of surface-active ingredients from the pulp, such as tall oils, soaps, fibers and particles. Many different types of antifoamers have been developed and these are utilized in the different processing streams and enable paper mills to run at higher speeds with greater efficiency and capacity. It was for the pulping process that black-liquor antifoamer compounds were formulated based on hydrophobic silica in hydrocarbon oil. Today, modern paper mills need easy-to-pump, easy-to-mix, stable-on-storage and cost-effective antifoamers, and between one-third and one-half of the total amount of antifoamer chemicals manufactured are used in this industry. Some of the major problems caused by foaming in paper mills are indicated in Fig. 10.1.

Many other types of industrial processes in which agitators, distillation columns, pipes, boilers, water discharges and so on are used need antifoamers to ensure high process efficiency and reduce environmental problems. At present the most effective and versatile chemical antifoamers are often mixed formulations. In fact, modern commercial formulations often contain mixtures of silicone oils, silicone surfactants or silica gels with possibly two or more types of dispersed hydrophobic aggregates (with sizes around 1 μm, specific gravity 1.0–1.3, with rough fractal shapes). These mixed-type antifoamers are widely used and are very effective at low concentrations

(10–1000 ppm). The particles may be hydrophobized silica or glass and are often referred to as the "activator," with the hydrocarbon or polydimethylsiloxane (PDMS) liquid or oil being referred to as the "carrier." Due to their low surface tension, silicon oils were also originally used in non-aqueous foam systems such as gearbox oils and hydraulic fluids, but they had disadvantages in that they had a negative effect on air release; today the problem has been solved by the use of organomodified siloxanes.

However, less expensive single-system antifoamers are frequently used in aqueous foams, and these exist in many different forms such as soluble liquids, insoluble liquids, oils, gels, hydrophobic particles, emulsions and microemulsions. A typical list of single-system chemical antifoamers might include tributyl phosphate (TBP), PDMS, silicone fluids, alkyl amines, amides, thioethers, mineral and vegetable oils, waxes, fatty acid esters ("Span 20"), alcohols (octanol), fatty acids and their derivatives (tall oil, aluminum stearate, and the calcium, aluminum and zinc salts of fatty acids) and many other different types of particles. Cheaper chemicals can also be employed, such as glyceryl esters in the form of "pork," fat or butter and also synthetic esters of polyhydric alcohols. The patent literature is extensive and contains a wide range of chemicals. Recently, ionic liquids, such as phosphonium-based chemicals, have been evaluated with regard to their defoaming performance by Cytec Industries, USA (6).

One of the essential requirements for antifoams is to produce droplets that enter the air/liquid interface; this requires a fairly low surface tension. This is not difficult to achieve with water-based foams, but for non-aqueous foams, only specific surfactants based on silicon oils can be used. The surface tension of a typical liquid hydrocarbons is usually about 30 mN/m, and since the silicones give considerably lower surface tension values, they can easily enter the air/hydrocarbon interface. In addition, they are chemically inert and have a lower density than water and lubricating oils. They are also effective since they have longer lifetimes because they are incompatible with oils and are involatile. PDMS is frequently used for inhibiting foam in the petroleum industry. Other special polymers such as fluorosilicones and perfluorinated hydrocarbons give extremely low surface tensions; these are also effective in non-aqueous foams, but they are expensive. The physico-chemical properties can be easily modified by changing the chain length of the cation or by changing the type of anion to produce different levels of hydrophobicity. A classification of chemical and physical defoaming methods is summarized in Fig. 10.2.

In considering the economics, antifoamers are usually budgeted as the cost per unit of product manufactured, for example, the cost per liter of paint, the cost per ton of paper or the cost per batch of chemicals produced. In many cases, this results in the use of relatively small amounts of expensive antifoamers, thus leading to a lower cost per unit product. In other situations, although more expensive antifoamers such as silicon polymers may be more efficient, the wastage may be high, so it is often cheaper to use less expensive antifoamers such as vegetable or mineral oils. Many industrial suppliers install specialized monitoring equipment to achieve minimum defoamer consumption. Many of these will be discussed in detail in the following sections.

Fig. 10.2 Chemical and physical methods of foam breaking. From ref (5).

10.2 Physico-chemical mechanisms

As such a diverse range of antifoaming chemicals are used for different processes, it is not surprising that so many alternative mechanisms have been proposed to explain their action, and extensive experimental studies dealing with the basic mechanisms of antifoam action have been reported. The situation in reality is far more complex, and it appears that in some systems there may be several different mechanisms occurring concurrently. However, the main function of the antifoam is to replace or reduce the amount of surfactant at the interface with something that leads to a less stable foam film. The chemical must also be insoluble in the foaming medium but resistant to chemical degradation. On a fundamental level, the mechanisms of the silicon oil-based compounds are possibly the most well understood due to a considerable effort by Denkov and coworkers (7).

10.2.1 Droplets and oil lenses: spreading coefficient (S_c), entry coefficient (E_c) and bridging coefficient (B_c)

Many liquid antifoamers form undissolved oil droplets on the surface of the foam film, and this can successfully lead to film rupture. Chemicals such as alkyl phosphates,

alcohol, fatty acid esters and polydimethylsiloxanes are included in this group. Several possible mechanisms have been suggested to explain film rupture by antifoaming droplets or oil lenses. A widely accepted mechanism for the antifoaming action is that the process first involves the oil drop entering the air/water interface and, in a secondary step, beginning to spread over the foam film, leading to rupture. Based on this approach it was found convenient to introduce an entering coefficient (E_c) and a spreading coefficient (S_c) which have been defined in terms of the change in free energy when the oil droplet enters the interface or spreads at the surface. These are expressed as follows:

$$E_c = \gamma_{w/a} + \gamma_{w/o} - \gamma_{o/a} \tag{10.1}$$

$$S_c = \gamma_{w/a} - \gamma_{w/o} - \gamma_{o/a} \tag{10.2}$$

where $\gamma_{w/a}$, $\gamma_{o/a}$ and $\gamma_{w/o}$ are the equilibrium interfacial tensions of the aqueous phase and oil phase and the interfacial tension of the oil/water interface, respectively. It is important to note that the entering and spreading coefficients are thermodynamic properties, which determine whether the particular configuration of the oil droplet is energetically favorable and are not related to the kinetics of the process that exist in the draining film. In fact, higher positive values do not always correlate with faster entering or spreading, but it merely indicates the ultimate thermodynamic situation. Silicone foam control materials entering the air/water interface are virtually always positive because the surface activity of silicones is higher (lower surface tension than the foaming liquid).

After entering the air/water interface, it was originally assumed that the oil drop must spread as a duplex film on each side of the original film. This acts to drive out the original liquid film and leaves an oil film which may become unstable to break-up. Clearly, two important steps need to be considered, since the mechanism is only feasible under certain critical conditions. These can be defined by $E_c > 0$, where the oil enters the air/water interface, and $S_c > 0$, where the oil spreads on the duplex film on each side of the original film. This situation is illustrated in Fig. 10.3, where the balance between the relevant surface tension and spreading coefficient is indicated.

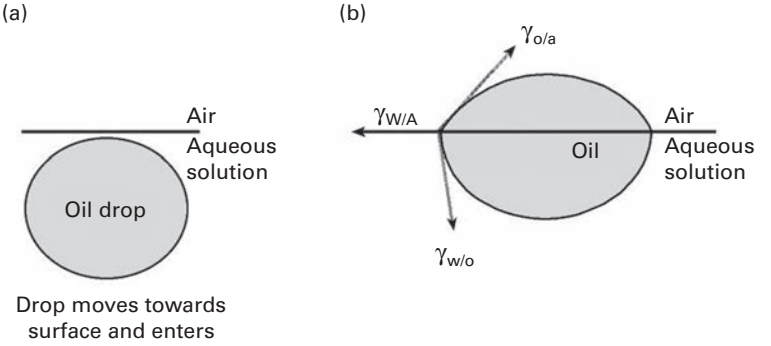

Fig. 10.3 (a) Entry and spreading of oil droplet at the air/solution interface; for successful entry $E_c = \gamma_{w/a} + \gamma_{w/o} - \gamma_{o/a} > O$ and (b) for successful spreading of oil droplet $S_c = \gamma_{w/a} - \gamma_{w/o} - \gamma_{o/a} > O$.

It was also originally assumed that it is purely the mechanical action of the spreading liquid which ruptures the aqueous foam film and that as the lens slips over the underlying liquid the lateral stress to the liquid below transfers a shearing stress to a depth of several microns. This causes the adjacent liquid to move in the same direction, and such liquid movement induces a thinning which increases the probability of rupture. However, although these equations and quantification of E_c and S_c are useful, in that they give a rough guide to antifoaming action, they are generally considered to be inadequate. In fact, they do not consider the geometry of the system or the interactions of thin film forces, and another possible explanation for the unreliability of these spreading equations is that there is a difference in magnitude between the initial entry coefficient (where the components are pure) and the equilibrium values (where contamination often occurs).

In addition, whether the simplified approach, in which the oil emerges from the interface to form a lens without contaminating the w/a interface (a partial wetting situation), occurs is still not clear and two additional situations have also been considered. The first involves the oil spreading at the w/a surface producing an unstable film which breaks up leaving oil lenses which contaminate the interface (pseudo-partial wetting). Alternately, the oil may spread to form a duplex film with no lenses where the film is so thick that the w/a and o/a surface tensions of the film have the values of the bulk phase (complete wetting). In each of these three situations, the equilibrium spreading pressure can be only either zero or negative; this leads to the oil drop bridging both sides of the aqueous film, causing instability and rupture.

Early work emphasized the importance of the formation of the oil lens (but not necessarily the spreading) in the mechanism of antifoaming, and it was only later that it was suggested that the oil lens could break the thin foam film by a bridging mechanism. The bridge stability depends primarily on the wettability of the bridging particle, and the bridging/dewetting mechanism is usually expressed in terms of the bridging coefficient B_c, which is related to the interfacial energies by the equation

$$B_c = \gamma_{w/a}^2 + \gamma_{w/o}^2 - \gamma_{o/a}^2 \tag{10.3}$$

From theoretical analysis, it was shown that positive values of B_c correspond to bridge dewetting, which is linked to the ability of the particles to bridge the foam films. It should be positive for the particle to act as antifoam. Several alternative types of mechanisms were originally suggested to explain film rupture with droplets – which are illustrated in Fig. 10.4 – but the bridge/dewetting mechanism is generally considered to be the most probable situation. In all these processes, initially $E_c > 0$ and this step is followed by a fluid entrainment or bridging process, which involves the antifoam oil spreading rapidly over the thin film lamella surfaces, and may cause a Marangoni-driven flow of liquid in the foam film (fluid entrainment). The enhanced drainage is due to capillary effects, and this can lead to film rupture through bridging the aqueous films by a dewetting mechanism.

The bridging/stretching mechanism was discussed by Denkov (7) based on an oil lens spanning a foam film that can stretch extensively before finally rupturing. Once the oil

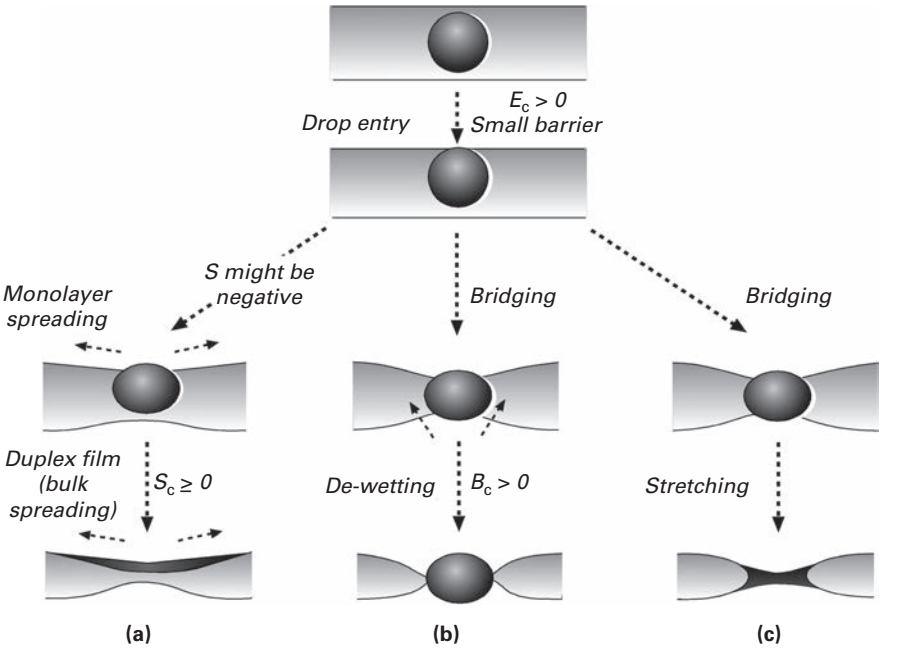

Fig. 10.4 Different types of mechanisms suggested for foam film rupture by antifoam droplet: (a) spreading-fluid entrapment which leads to a Marangoni-driven flow of liquid causing local thinning; (b) bridging dewetting; (c) stretching bridging. In all of the mechanisms, the first step is the particle entry, which requires a positive entry coefficient and a small force barrier.

bridge is formed, it eventually acquires a biconcave shape, with the thinnest region in the center. This bridge is unstable due to uncompensated capillary pressure at the w/o and o/a interfaces and stretching occurs in a radial direction. Eventually, the thin foam film in the center of the bridge ruptures. The bridge stretching mechanism usually functions with deformable antifoam globules rather than with high concentration of solid particles or polymerized gel particles. The timescale of the bridge dewetting has also been estimated based on the time required for the foam film to thin down to a thickness comparable with the particle diameter. The process involves the rapid movement of the contact lines along the particle surface, pushing the liquid from the vicinity of the particle.

In addition, it is important to consider the fact that in real applications, foam breakage is often triggered by mechanical perturbations and even vibrations. Although values of E_c, S_c and B_c can be determined from measurements of the interfacial tension, it is questionable if these models account for the rupture barrier of asymmetrical oil/water/air films which appear when the oil approaches the foam film surface. The size of the droplet relative to the film thickness is also important for the antifoamer to function, especially in the case where the droplet cannot directly enter the foam film and becomes entrapped and compressed in the Plateau borders (PBs). This has an important influence on the process kinetics, and several studies suggest that there is no direct relationship between the magnitude of E_c, S_c and B_c on one side and the antifoam efficiency on the other.

It is also often assumed that for effective antifoam action to occur, the antifoaming agent must be in the form of insoluble or undissolved particles or droplets which transfer to the interface. However, this is not necessarily the case since there is some early evidence that some antifoamers such as tributyl phosphate and methylisobutyl carbinol (MIBC) are effective in the solubilized state and can reduce the stability of sodium dodecyl sulfate (SDS) and sodium oleate surfactant-stabilized foam systems. The situation is somewhat unclear since the oils may slightly exceed the solubility limit and the emulsifier droplets of oil may then have an influence on the antifoam action. It has also been claimed that oil solubilized within micelles may cause a weak defoaming action. Mixed micelle formation with extremely low concentrations of surfactant may explain the actions of insoluble fatty acid esters, alkyl phosphates (esters) and alkyl amines. At present, there appears to be no complete explanation for the action, and while there are many cases which demonstrate that solubilized antifoams may reduce the foam stability in micellar solutions, there are also examples where dissolved antifoam can enhance foaming.

10.2.2 Emulsified droplets and pseudo-emulsion films

As early as 1994, Wasan and coworkers (8, 9) established that foam stability in the presence of emulsified droplets (in a micellar environment) was dependent on the stability of the thin film between the air/water interface and approaching drop. This was considered as a "pseudo-emulsion film" or "asymmetric film" and could be stabilized by various interfacial forces which suppress drop entry. The classical E_c for drop entry did not take into complete account the nature of the pseudo-emulsion film, for example, the influence of the geometry of the system on thin film forces. Lobo and coworkers (8) emphasized the role of the so-called pseudo-emulsion film on the stability of the aqueous foaming system. Different processes involving entry and spreading of the pseudo-emulsion film are outlined in Fig. 10.5.

Clearly, the classical entering and spreading coefficients cannot predict the dynamic changes in configuration of oil at the air/water surface and thus cannot predict the effect of oil on foam stability (i.e. even in the case of $E_c > 0$). The entry of the oil droplet into the air/water interface may be retarded by the interfacial forces, which may reduce the drainage rate of the film. In fact, the classical theories generally do not consider the excess pseudo-emulsion film energy. Important parameters that need to be considered include surface gradients at the interface and the surface viscosity of the film, as well as thermodynamic quantities such as disjoining pressure and film stratification. Further, the emulsified oil droplets may also accumulate within the Plateau borders of the draining foam films and inhibit the drainage, as indicated in Fig. 10.6.

10.2.3 Effects of disjoining pressure on the stability of the pseudo-emulsion film

The entry of the droplet into the interface is dependent on drainage and stability of the oil/water pseudo-emulsion films which are governed by the electrostatic and steric contributions inucluded in the disjoining pressure isotherms. In 2003, Bergeron, and

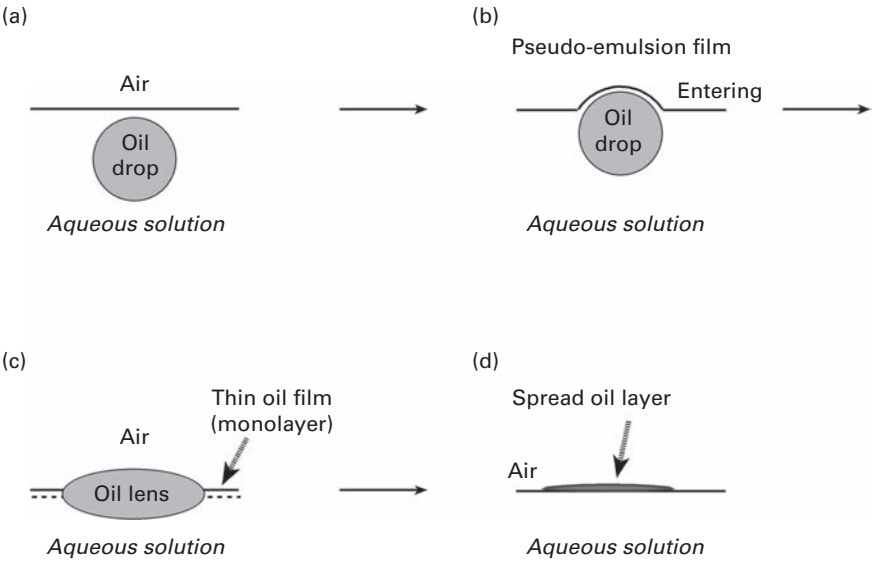

Fig. 10.5 A macroemulsified oil system showing the configurations of the oil at the gas/aqueous interface: (a) oil drop inside the solution; (b) oil drop at the surface separated from the gas phase by a pseudo-emulsion film; (c) oil lens; (d) spread of oil layer at the solution surface. The pseudo-emulsion film is unstable, thus enabling the oil to spread on the surface. From ref (9).

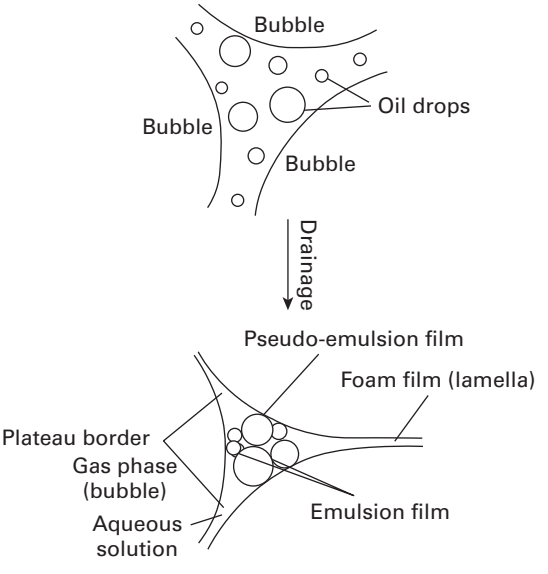

Fig. 10.6 Schematic representation of a microemulsified oil system. The drainage of the film may be reduced due to accumulation of emulsified oil droplets within the Plateau borders. The formation of both the emulsion and the pseudo-emulsion films is indicated. The factors affecting foam stability were found to be oil volume, drop size and oil phase density. From ref (9).

coworkers (10) introduced a generalized entry coefficient E_g instead of the classical E_c. This was defined by the equation

$$E_g = -\int_0^{\Pi_{AS}(h_E)} h d\Pi_{AS}(h) \tag{10.4}$$

where $\Pi_{AS}(h)$ is the disjoining pressure of an asymmetric film at thickness h and h_E is the equilibrium thickness at a certain capillary pressure. In order to evaluate E_g knowledge of the disjoining pressure isotherm for the asymmetric pseudo-emulsion film is required. According to this equation, a negative E_g defines the system as non-entering and a positive one defines it as entering. Both the electrostatic and steric repulsion forces act to reduce the value of E_g and can cause it to be negative even though E_c is positive. An alternative approach was proposed by Gao and coworkers (11) in which a molecular dynamic theory was used to describe the oil bridge stretching mechanism of foam rupture. In this model, the stretching forces were divided into three parts: the initial increase in the force, the middle equilibrium stretching force, which stretched the middle of the oil bridge and the final decreasing force. It was suggested in this study that bound water connecting the head groups of the surfactant through hydrogen bonding played a role in the instability of the pseudo-emulsion film and could hinder the disappearance of the water phase in the film. The horizontal stretching force which stretched the oil bridge was also found to be dependent on the properties of the oil molecules. However, since the capillary forces and disjoining pressure were mimicked by arbitrary forces, Garrett (2), in 2015, questioned the validity of this type of approach.

In commercial antifoams, the rupture of the pseudo-emulsion films is usually achieved by adding hydrophobic particles to the oil which causes the rupture by a bridging mechanism similar to what occurs with hydrophobic particles in foam films. However, the situation is complex and alternate theories have been considered. For example, Shu and coworkers (12) studied the precipitation of oleic acid drops from sodium oleate solution in the low pH region which caused a reduction in both foamability and foam stability. These workers explained defoaming by the bridging effect of the oleic acid droplets and also showed that the removal of the droplets by increasing the pH increased the foamability. However, these workers did not consider the equilibrium phase diagram for the sodium oleate/oleic acid systems which has been extensively studied by Pugh (13) for the flotation of minerals. In fact, it has been established that several different types of monomeric and dimeric surface-active species which may play a role in the stability of the bubbles are present in the solution.

10.3 Experimental studies

It is sometimes difficult to determine whether E_c, S_c and B_c are positive or negative for many more complex liquid antifoam droplets (consisting of polar oils rather than

silicones) or to correlate these values to foam stability. In 2003, Zhang and coworkers (14) studied the stability of foams generated from several ethoxylated alcohols (at 0.01 wt% concentration) with dispersed drops of *n*-hexadecane, triolein or mixtures of these oils. Initially, only small amounts of oleic acid and negligible amounts of Ca^{2+} were present in the systems. An attempt was made to analyze these systems in terms of E_c, S_c and B_c, ($E_cS_cB_c$ analysis), and although some degree of success was achieved with some systems, in other cases only a limited amount of success was achieved. This was explained by strong repulsion interactions caused by overlapping electrical double layers in the asymmetric oil/water/air film (the pseudo-emulsion film) which prevent the oil from entering the air/water interface.

In further experiments by Zhang and coworkers (14), it was found that calcium soap was precipitated (by the reaction of fatty acids in the oil with Ca^{2+}) in mildly alkaline conditions which coated the oil drops. It was suggested that the combination of oil and calcium soap particles produced a synergistic effect facilitating the well-known bridging instability of foam films. This bridging was sufficient to overcome the repulsive disjoining pressure in the film, and for both surfactants with the triolein/oleic acid mixtures, the values of E_c and B_c (in the presence of calcium soap) were found to be positive shortly after foam generation but became negative under equilibrium conditions. These results are consistent with the experimental observation that most antifoaming action occurred shortly after foam generation.

10.4 Surface tension gradients, viscosity and drainage

Spreading is usually driven by a surface tension gradient between the spreading front and the leading edge which cause a shear force dragging the underlying liquid away from the source, and several different types of antifoam materials may function by this mechanism: for example, (a) droplets/solids or liquids containing surfactants other than those stabilizing the foam, (b) liquids which contain foam stabilizers at higher concentrations than that which is present in the foam and (c) the vapors of surface-active liquids. Chemicals which are dispersed in the liquid will emerge at the thin film interface as a lens causing a lowering of the viscosity and an increase in the drainage which generally leads to a decrease in stability. These groups included chemicals which may (a) reduce the bulk viscosity increasing the drainage or (b) reduce the surface viscosity and elasticity. In the latter case, the surface elasticity may be eliminated by a swamping of the surface layer with an excess of the lower viscosity compound. If the compound is soluble then a sufficient amount must be added to exceed the solubility limit. The insoluble monolayer cannot provide any elasticity, although this can be achieved by the soluble monolayer in equilibrium with the solubilized chemical.

One of the early more general theories suggests that the spreading film of antifoam may simply act to displace the stabilizing surfactant monolayers. As the oil lens spreads and expands on the surface, the tension will be gradually reduced to a uniform level which may cause elimination of both the stabilizing surface tension gradient and the surface elasticity. There are several other different mechanisms for reducing the surface

viscosity, depending on the conditions in the surface layers. For example, many low molecular weight bulky surfactants, such as tributyl phosphate or some non-ionic surfactants can be used to reduce or disrupt the cohesion in the layer and such effects depend on the molecular structure of the additive. Other material may not be surface active but may act as a co-solvent and thus reduce the concentration of surfactant in the surface layer. Unfortunately, frequently fairly large quantities are needed (e.g. 10% ethanol or methanol) but smaller amounts of low molecular weight (short-lasting) antifoamers can be applied by spraying the solution. Clearly, this is a more economical approach. In addition, although small amounts of solubilized dodecanol may increase the foam stability of an anionic surfactant in water, a like quantity of solubilized octanol will have a contrary effect. This may be explained by the octanol rapid diffusing to the surface, reducing the dynamic surface tension and allowing less time for a Gibbs–Marangoni effect to function.

10.5 Superspreading

Several studies suggest that antifoaming is related to either "polymolecular spreading" or "superspreading" which involve the acceleration or transformation of non-stable polymolecular films into lenses. The spreading of antifoamers is rather complex, and nonionic trisiloxane surfactants have been reported to show superior wetting properties, particularly on hydrophobic surfaces. These surfactants not only have low surface tensions but also a tendency to form bilayers, which can aggregate into lamellar vesicles (15). Based on the molecular packing, there is a fundamental difference in spreading behavior at the interface of a micelle-forming surfactant and of a vesicle-forming surfactant. Models for spreading have been suggested from experiments of the spreading kinetics of ethoxylated and propoxylated trisiloxane surfactants on a polypropylene substrate.

10.6 Influence of the interfacial and micellar aggregates

It is well known that certain antifoams such as methyl or ethyl alcohol, when added to the foaming solution, can change the CMC or solubility of the surfactant and thus indirectly affect the adsorbed layer. In fact, detailed studies by Jha and co-workers (16) clearly emphasized the relationship between the stability of a surfactant micelle and the stability of the foams. From experiments carried out with foam stabilized by SDS, it was shown that several chemicals, such as 2-ethylhexanol (EH), tributyl phosphate (TBP) and tetrabutylammonium chloride (TBAC), can change the stability of the micellar aggregates, thus leading to changes in the stability of the foam systems. In these studies, the stability of micelles was determined from the micellar relaxation times, as measured by pressure jumps. As the antifoam concentration increases, the micellar relaxation time also increases (indicating increasing micellar stability) until a critical concentration is reached.

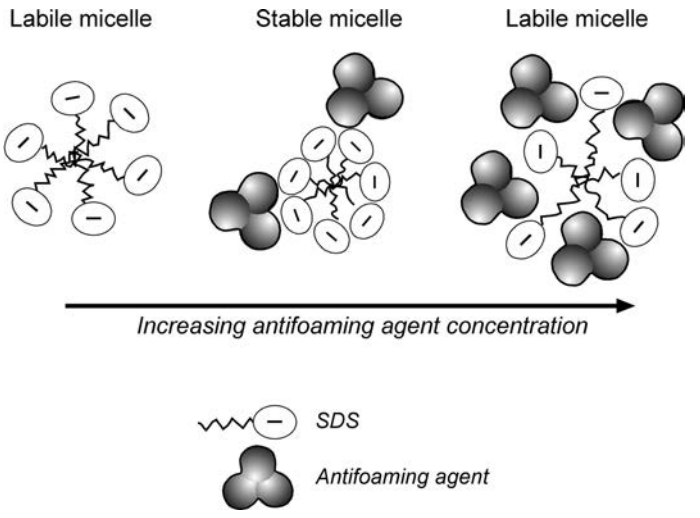

Fig. 10.7 Schematic of the microstructure changes for SDS micelles on the addition of an antifoaming agent. From ref (16).

Further increases in antifoamer lead to a decrease in the micellar relaxation time (indicating a decrease in micellar stability). The initial increase was attributed to the promotion of the micellar stability by the added chemicals, which minimized the repulsion between the head groups of the SDS molecules at the micellar surface or at the interface. Two opposing effects were considered depending on the concentrations of antifoamer, and the type of antifoaming agents that can stabilize the SDS micelle at lower concentrations and in turn act as a foam inhibitor. However, beyond a critical concentration, the antifoaming agents destabilize the micelle, which then begins to improve the formability of the SDS. The changes in the microstructure for SDS micelles on the addition of an antifoaming agent are shown in Fig. 10.7.

Certain types of cationic organic electrolytes have also been shown to destabilize foams generated by anionic surfactants. Blute and coworkers (17) generated foams with sodium dodecyl sulfate surfactant and added a series of different types of tetra-alkyl ammonium (TAA) ions to suppress the foaming. The extent of foam reduction was found to be dependent on the electrolyte/SDS ratio. Based on the Gibbs adsorption isotherm and surface tension measurements, it was found that the organic salts caused an increase in the intermolecular area of the adsorbed species which in turn increased with an increase in the size of the cationic salt. The foam suppression was explained by a complex formation caused by the interactions of the anion with the cation which reduced the surface viscosity. The CMC of the SDS solution was also reduced with increase in size of the organic tetra-alkyl ammonium ion. In Fig. 10.8, the half-life of the foam (the inhibiting effect) for the different organic salts versus the ratio of electrolyte/SDS ratio in the presence of an inorganic electrolyte (NaBr) is illustrated.

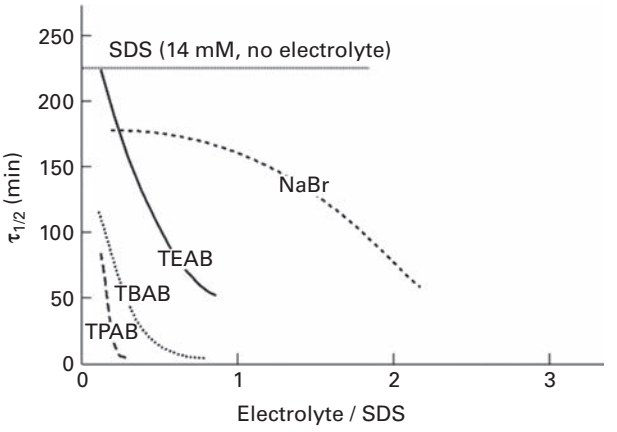

Fig. 10.8 The half-life of SDS in the presence of different organic electrolytes versus the electrolyte/SDS molar ratio. The electrolytes are tetrapentylammonium bromide (TPAB), tetrabutyl ammonium bromide (TBAB) and tetraethyl ammonium bromide (TEAB). Also shown is the plot for an inorganic electrolyte and sodium bromide (NaBr) for comparison. The SD concentration was 14 n mm. The foams were generated by the Ross–Miles procedure. From ref (17).

10.7 Particles

Solid particles that have a reasonably high degree of hydrophobicity (e.g. coal dust, sulfur, non-wetting quartz, etc.) usually exhibit a finite contact angle when adhering to an aqueous interface and may cause destabilization of foams. Many practical examples of such behavior can be found in mineralized froths, but the mechanism may not necessarily involve wetting, since hydrophobic silica can deplete the stabilizing surfactant (through rapid adsorption), causing weak spots in the film. In earlier studies, there was a tendency to try and emphasize the importance of wetting by correlating an increase in contact angle with an increase in defoaming action. However, some of the experimental data are probably erroneous due to the difficulties of measuring contact angles and the influence of the shape and roughness of the particles on the foaming action. Other studies have been reported in which foaming was related to the degree of wetting of the inert particles; this correlation led to the idea of a particle bridging mechanism (a similar mechanism as for the oil droplets) causing rupture of the thin film. Garrett (18) reported a series of shake-test experiments with finely divided (~ 5 μm) PTFE particles as the antifoam material. A reasonable correlation between the foam volume destroyed and the receding contact angle was found from this study. The antifoam action for these spherical particles has been related to the wettability, contact angle and the bridging characteristics for many systems. However, for particles with rough edges, the situation then becomes somewhat more complex. Johansson and Pugh (19) studied the stability of foams in the presence of finely ground quartz particles of different size fractions. In this work, the surfaces of the particles were methylated to produce a range of hydrophobicities. Both the dynamic and static froth stabilities were then determined in a glass

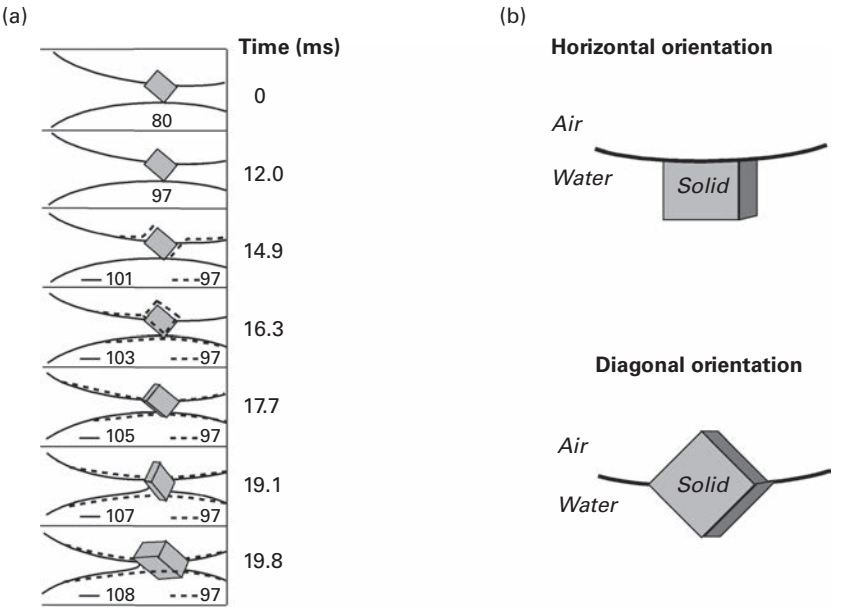

Fig. 10.9 (a) Sequence taken from high-speed photography experiment showing the interaction of cubic galena particles in a thinning film. From ref (20). This demonstrates the importance of the contact angle on the film rupture. The latter can occur as the bubble can bridge both surfaces of the film, whatever the contact angle. With cleaved surfaces, the contact angle gives only a rough guide to stability. (b) Orientation of the cleavage plane can occur in, or diagonally to, the surface. Stable films will interface and thus allow easy movement of the three-phase contact. In this diagonal orientation, as the film thins the aqueous phase peels off the particle to form a hole.

column. From this study, the concept of "maximum enhanced foam stability," which corresponded to a critical surface hydrophobicity, shape and size was established.

In 1982, the mechanism of film collapse by a single spherical and a cubic particle passing through a film was studied in cinematographic experiments carried out by Dippennar (20, 21), and the results generally confirmed Garrett's dewetting mechanism, but it was found that the dynamic contact angle, rather than the equilibrium situation, was more relevant. Fig. 10.9(a) shows the sequence of events of a galena particle passing through the film. This is particularly of interest since usually foams are generated through non-equilibrium processes and the air/water interface expands rapidly. From this study, Dippenaar (20, 21) also concluded that orthorhombic hydrophobic particles could adapt two orientations (diagonal and horizontal) at the interface, as illustrated in Fig 10.9(b), but only the diagonal orientation gave rise to foam rupture with a mechanism analogous to spheres. Further experiments carried out with galena (cubic shaped particles) also showed that with contact angles < 90°, the froth was easily destabilized, and this was explained by the ease of movement of the three-phase boundaries across the smooth regular surface. All of these studies more or less verify the influence of the size, shape and hydrophobicity of the particle on the foam stability. In fact, the particle

characteristics also govern the degree of penetration into the individual foam films and the movement of the three-phase boundary along the surface. In addition, it demonstrated that the number of particles in the froth also played a role in stability (providing the particles were of uniform hydrophobicity and shape).

Almost 50 years later, Morris and coworkers (22) revisited this early study by Dippenaar (20) and carefully re-examined the data. Examination of the original film data frames revealed that the aspect ratio of the orthorhombic particles is about 1.4 with the contact angle falling between 72° and 88°. The experiments were repeated with similar hydrophobic galena particles with the contact angles was between 70° and 90°, but in this case the aspect ratio was unity. In addition, modeling and theoretical studies were carried out to compare the experimental data. Based on a surface energy minimization analysis which makes use of the alternative surface evolver software developed by Brake (23), the relative work of adhesion of the particles to the interface was calculated, which further enabled the surface energy profile of particles as a function of orientation to be calculated. The model was based on 20 particles randomly packed in the liquid film, and the capillary pressure required to rupture the film for specific combinations of particle arrangements, packing densities and contact angles were identified. Although the profile revealed a surface minimum which was consistent with a stable orientation, it was also shown that four different orientations were possible for an orthorhombic particle bridging the foam film. These were designated as vertical, horizontal, rotational and diagonal. As expected from these calculations, the particle adopted a rotational orientation, although no apparent observations of either horizontal or vertical orientation was observed. From the experiments and modeling it was concluded that the liquid vapor interface was highly distorted around the particle, and under certain conditions, the film surfaces were drawn together behind the particle, thus causing rupture. This mechanism was quite different from the bridging mechanism suggested by Dippenaar (20).

In an attempt to study the different behaviours between the solid and the emulsified liquid states of the particles or droplets in defoaming, several thermal (melting) investigations have been carried out using hydrocarbon particles. Triglycerides and long-chain fatty acids with melting points < 100°C have been frequently used and dispersions were prepared by first emulsifying the molten material and then cooling below the melting point. Experiments have demonstrated a sharp deterioration in the antifoaming effectiveness occurring in the region of the melting point transition for paraffin waxes in sodium alkylbenzene sulfonate solution. At higher temperatures, where the entire solid is converted to liquid, the antifoaming performance was reduced. This behavior has been explained by the solid particles having a more irregular shape, with sharp and rough edges and apexes, producing finite contact angles under dynamic conditions. As the wax melts, the edges are removed and the particles become more symmetrical, enabling a bridging mechanism to come into play.

The practical aspects of using specifically shaped particles in defoaming were highlighted by Frye and Berg (24) in 2006 from experiments in which a hydrodynamic analysis of the mode of action of smooth-shaped, inert, solid hydrophobic particles (spheres, discs, rods and ellipsoids) was made on thin films. It was concluded that for

dewetting and rupture to occur, the receding contact angle must be > 90°, while to achieve rapid film rupture and high breakdown rates, an extra 5° or 10° over this critical angle was required. However, in "foamy" solutions, these values were found to be very difficult to achieve, and it was suggested that it was then preferential to use rough-shaped particles, which gave sharp angles. In 2006, Vijayaraghavan and coworkers (25) studied the foaming behavior during evaporation of solutions containing irregularly shaped, fine crystalline particles of sodium chloride which were hydrophobized by the physical adsorption of a cationic surfactant. In this system, the partially wetted particles were found to be responsible for foaming, and conventional silicone/hydrophobic particles failed to reduce the foaming. It was also shown that the addition of chemical flocculant further reduced foaming through aggregate formation.

10.8 Cloud-point antifoamer: block copolymers

Nonionic ethoxylate and propyloxylated surfactants and block copolymers such as PEO-PPO-PEO or PPO-PEO-PPO types, "Pluronics" and poloxamers are used as antifoamers in a wide range of applications, for example, in textiles and dishwashing. The polarity of these copolymers depends on the ratio of the PEO (hydrophilic) and PPO (hydrophobic) components. They are fairly soluble in water at low temperatures but partially miscible at higher temperatures, and above a critical temperature known as the cloud point (CP), the micellar solution undergoes a phase change to form two conjugate micellar solutions, one dilute and the other concentrated. The CP is the temperature at which droplets of the concentrate conjugate phase separate causing the solutions to become turbid. In these systems, the CP can be changed by altering the PEO/PPO ratio. Usually, these nonionic compounds are added to an aqueous solution of a foaming surfactant to produce an antifoam effect at temperatures near or above the cloud point, but in some cases the CP may increase or even become eliminated due to the formation of mixed micelles. Other commercial surfactants, such as Triton XI00, OP-10 and DC-10, behave in a similar manner, with liquid drops being observed in solutions above the CP. It has been suggested that the antifoam mechanism is based on a film-bridging mechanism associated with the phase change and droplets.

10.9 Fatty alcohol antifoamers: melting point, gel layers and droplet rigidity

In the pulp and paper and detergent industries, it is sometimes desirable to avoid the use of antifoams with silica hydrophobic particles or silicon oils and instead use a water-based fatty alcohol formulation which is more environmentally friendly. In 2006, Joshi and coworkers (26) carried out experiments with antifoam mixtures consisting of long-chain (C_{14}–C_{30}) alcohols. Antifoaming tests were carried out with aqueous foaming solutions formulated from a mixture of a nonionic surfactant, polysaccharides and

preservatives. Two types of alcohol suspensions were tested, as antifoamers, one with fatty alcohol particles with a low melting point (31 to 52°C) while the other contained fatty alcohol particles with a high melting point (> 65°C). The low melting point particles were shown to be increasingly effective with increase in temperature, but became inefficient at higher temperatures (> 60°C). This deteriation in performance was possibly due to the particles melting and changing shape. However, the higher melting antifoam particles which remained solid were found to act effectively as antifoamers at this higher temperature.

Although the cloud point action plays an important role in determining the antifoam efficiency of polymer drops, the rigidity of gel layers on the adsorbed polymer droplet also needs to be considered. This can impart strength to the drop, which strongly influences the coalescence (stability) of bubbles. In 2005, this type of antifoaming action was demonstrated by Joshi and coworker (27a) from foam studies with water-based ethoxylated and propoxylated straight-chain fatty alcohol dispersions. These surfactants form gel-like phases which exhibit viscoelastic properties in concentrated solutions. Foams were generated using the cylindrical glass column attached to a recirculation system containing an aqueous solution of polysorbate 20 surfactant (as a model for an industrial white water-foaming suspension). With increased temperature from about 13 to 26°C, foaming increased (attaining a maximum at 26°C), but it decreased at higher temperatures. In addition, using a two-bubble coalescence technique involving a CCD camera, the coalescence behavior of two block copolymer droplets suspended from opposing capillaries was recorded. From these tests, it was observed that the drop coalescence decreased as the temperature increased from 25 to 60°C. Also, the bulk viscosity and interfacial rigidity (determined using an oscillatory thermo-rheometric method) decreased with temperature (through the same temperature range).

From additional experiments using small-angle X-ray scattering, micro-differential scanning calorimetry and proton nuclear magnetic resonance, the formation of ordered gel-like structures on the droplets was confirmed. This study demonstrated that the deformation of the droplet or weakening of the interfacial gel caused a decrease in coalescence and increase in foaming. The gel appeared to be squeezed out from the region of contact between the two bubbles, as indicated by the dotted ellipse in Fig. 10.10. Droplet deformation was also shown to be facilitated by the reduction in bulk viscosity. Furthermore, foaming experiments with a sparged air foam column showed a significant enhancement in antifoaming efficiency when highly hydrophobic particles are embedded in the BCP drops dispersed in water.

These experiments were extended by Joshi and coworkers (27b) which revealed the influence of the process dynamic and surfactant gradients in these types of defoaming systems. These workers formulated an antifoamer system by dispersing fatty acid particles in ethoxylated alcohol solution, and the mixture was then added to a second surfactant solution which caused an antifoam effect. Two colliding air bubbles in a liquid pool in the presence of the antifoam were also observed visually, and it was found that the action of the surfactant in the antifoam action involved a surface tension gradient due to the local differences in surfactant concentration. This resulted in a reverse flow and

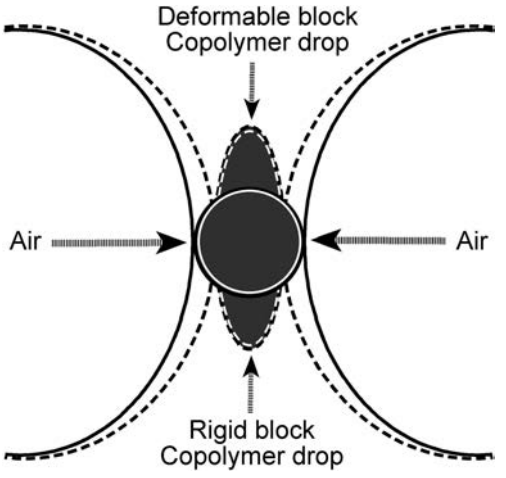

Fig. 10.10 Deformation of co-polymer drop reduces its ability to bridge two bubbles and break the thin aqueous film reducing the coalescence (antifoaming efficiency). From ref (27).

desorption of surfactant from the fatty alcohol particles. The surfactant-laden hydrophobic particle located on the bubble surface moved from the periphery of a liquid film between two colliding air bubbles to their region of contact. Subsequently, the particle bridge and dewets the bubbles, resulting in film rupture. The rate of drainage of the liquid film depends on the particle hydrophobicity, which necessitates complete surfactant desorption from the particle surface. Drop volume tensiometry and macroscopic foam column experiments appeared to substantiate this observation.

10.10 Precipitation effects

The precipitation (removal) of the foaming surfactant from solution can reduce foaming, which may be further reduced provided the precipitated particles are sufficiently hydrophobic. For example, cationic surfactants added to foam stabilized by anionic surfactants can break-down the foam. Alternatively, foams stabilized by anionic surfactants can be destroyed by the addition of an oppositely charged inorganic species or near-stoichiometric concentrations of metallic ions to form insoluble salts. For example, fatty acids and their derivatives (tall oil, stearate, etc.) can be precipitated by the addition of calcium, aluminum and zinc salts (forming insoluble salts of the acids). There have been several attempts to relate the defoaming action to the solubility product of the precipitated particles. A typical series of results presented by Garrett (1) for metal oleates is shown in Fig. 10.11.

Zhang and coworkers (28) studied the kinetics involved in the precipitation of hydrophobic calcium oleate particles from fatty acid soaps in slightly alkaline solution and related this to the consequential defoaming behavior. In the experiments, reasonably stable foams were generated with two freshly prepared surfactant solutions (sodium

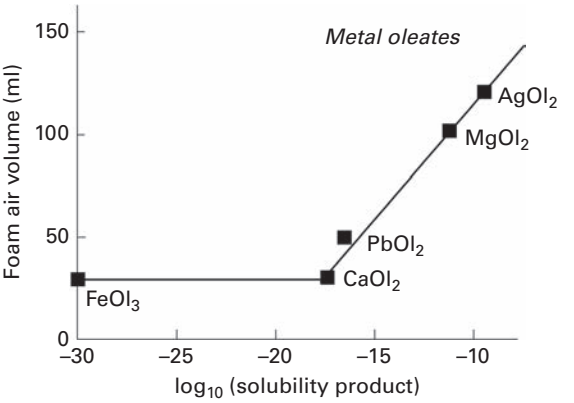

Fig. 10.11 The importance of the solubility product of the particles in defoaming, as shown by a plot of the froth air volume versus the solubility product of various metal oleates (2×10^{-5} *M* in a 10 mg dm^{-3} commercial foaming solution). From ref (1).

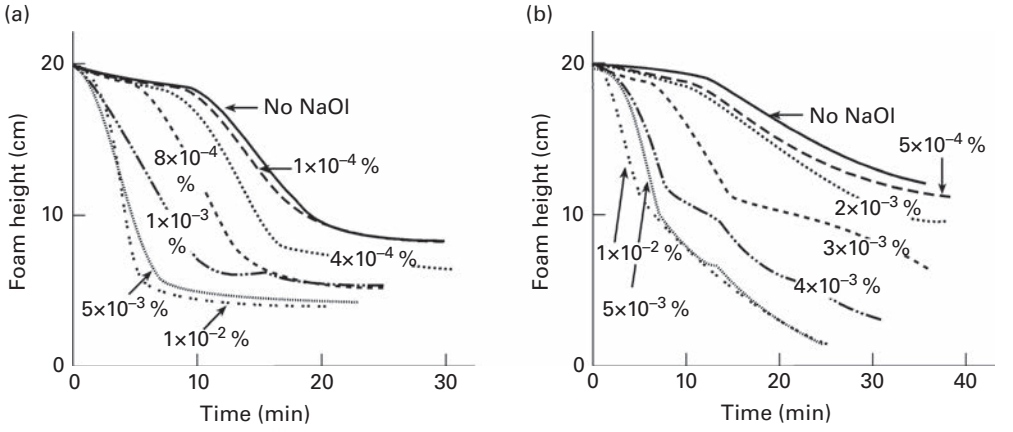

Fig. 10.12 (a) Foam stability with an anionic surfactant (a commercial alkyl ethoxyl sulfate salt designated NS–3S at 0.01%) at different concentrations of sodium oleate and (b) the foam stability with non-ionic surfactant (alcohol ethoxylate designated N25–7 at 0.1%) at different concentrations of sodium oleate at pH 9 and 300 ppm Ca^{2+}. From ref (28).

oleate and a nonionic) with a calcium hardness level of 300 ppm. However, the foam stability decreased with increasing concentrations of oleate. Kinetics effects were also demonstrated by using lower concentrations of oleate, and the defoaming action was found to be much slower during the initial stages of foam generation. Similar trends were observed for the nonionic surfactant but higher concentrations of surfactant were required to generate foam. In Fig. 10.12, the change in foam height is shown at increasing concentrations of oleate for both surfactant systems.

From further studies involving foam film drainage, experiments were carried out using a Scheludko–Exerowa cell (shown in Chapter 3), and it was suggested that a bridging defoaming was responsible for thin film rupture in the fresh solutions. At high dissolved oleate concentration (close to supersaturated), incorporation of the oleate and Ca^{2+} into the surfactant monolayers decreased the repulsive disjoining pressure interaction, producing unstable thin films. A simple model was used to estimate the oleate concentration at which precipitation commenced in the anionic surfactant solutions containing Ca^{2+}. The precipitation and aging effects appeared to be quite general, and even precipitates of polyvalent metal ions with long-chain alkyl phosphates, as well as carboxylates that may be combined with mineral oil or PDMS, can produce a synergistic antifoaming effect. This is a relatively inexpensive method of breaking foam, but unfortunately, due to the formation of solid contaminants and the adverse consumption of chemicals, precipitation defoamers are less frequently used in industry. Crystalline precipitates which exhibit a finite contact angle are also believed to cause defoaming by a bridging dewetting mechanism, as in the case of the addition of excess counterions to a solution of sodium dodecyl sulfate which reduces the Krafft temperature (29). The addition of counterions such as Ca^{2+} to double-chain surfactant sodium alkyl benzene sulfonate can cause the precipitation of a mesophase dispersion which also acts as a defoamer, and this has been used in detergency to eliminate residual foam during rinsing with hard water.

10.11 Mixtures of particles and oils

The synergistic antifoaming effect of mixtures of insoluble hydrophobic particles and hydrophobic oils (filled antifoams) when dispersed in aqueous media has been well established and reported in the patent literature since the early 1950s. Some examples taken from various industrial patents, which indicate the complex nature of the chemistry involved, are shown in Table 10.1. Most of these formulations have been developed by "trial-and-error" test methods.

The sizes of the particles are usually within the range 0.001–1 μm, with the solid content of the mixture being 1–20 wt%. One early idea for the role of the hydrophobic particles in the synergistic effect is that the spreading coefficient of the PDMS oil is modified by the addition of the hydrophobic particle. Garrett and coworkers (1) also suggested that oil/particle mixtures form composite entities where the particles can adhere to the oil/water surface. The particles alone may only show a weak antifoaming action (probably involving dewetting and bridging in foam films to form holes in a manner similar to that caused by the PTFE particles). However, the behavior of the particles in adhering to the oil/water interface may facilitate the emergence of oil droplets into the air/water interface to form lenses, thus causing rupturing of the oil/water/air films. This mechanism is similar to that of oil droplets forming mechanically unstable bridging lenses in foam films, where the configuration requires the rupture of oil/water/air films by particles, although the contact angle for rupture is less severe than that required for symmetrical air/water/oil films.

Table 10.1 Some examples, taken from the patent literature, of the synergistic antifoaming effect of various mixtures of hydrophobic mineral particles and silicone oils. From ref (1).

Oils claimed to be effective	Particles claimed to be effective	Actual examples given	Preferred concentration of particles (wt%)
Partially oxidized methylsiloxane polymer. May be diluted with dimethyl siloxane polymer and dispersed in benzene	Silica aerogel, presumably rendered hydrophobic by reaction *in situ* with the siloxane	As claimed	7.5
Methyl polysiloxane	Finely divided silica, presumably rendered hydrophobic by reaction *in situ* with the siloxane	Silica + methyl polysiloxane + emulsifiers	2–10
Silicone oils (product may be diluted by hydrocarbons, ethers ketones or chlorohydrocarbons, although this does not, however, appear as a specific claim)	Aluminum oxides, titanium dioxides, plus various silicas. These react with silicone oil *in situ*, with the reaction being catalyzed by an acid-condensation reagent	(1) Dimethyl polysiloxane + silica + aerogel + $AlCl_3$ diluted by toluene. (2) Dimethyl polysiloxane + alumina + $SnCl_4$ diluted by toluene (3) Dimethyl polysiloxane + precipitated silica + phosphorous nitrile chloride + poly(ethylene glycol) stearate.	1–30
Silicone oils	Pyrogenic or precipitated silicas, hydrophobized with "chemically bound methyl groups". Special reference is made to the relative ineffectiveness of the oil alone.	As claimed	2–8 (preferably 5)

In some systems several different antifoaming mechanisms may be operating. For example, water-borne coating formulations, often containing high volume fractions of latex particles together with high concentrations of surfactants, produce foams which are difficult to break using many other types of defoamers. In these systems, although the latex particles are too hydrophilic to adsorb at the air/solution interface and stabilize the bubbles, several interactions can play a role in controlling the stability/instability. For example, depletion of the surfactant concentration by adsorption on the latex particles will tend to reduce the stability, but also small mono-dispersed particles can produce a high viscosity and cause thin film stratification, which tends to increase the stability. However, sometimes particles are not efficient foam breakers where strong adsorbing foaming surfactants are present at high concentrations (> CMC), as in detergency, due to

the molecules adsorbing on hydrophobic particles, thus rendering them hydrophilic. In such cases, oil-based antifoamers are used. Garrett and coworkers (30) studied the foaming action of mondispersed styrene/acrylatex particles (100 nm diameter at 25 w % solids) using a mixed antifoamer consisting of hexadecane with hydrophobic silica particles (1 micron diameter at 10 w% solids). Strong antifoam was detected as resulting from the interaction of the larger silica particles/oil mixture with the smaller latex particles, producing an irregular structure which prevented stratification and increased drainage.

10.12 Fast and slow antifoamers and the film trapping technique

Prior to 2000, the antifoaming mechanisms of hydrophobic particles and silicon oil-based formulation was only partially understood, but post-2000 a considerable amount of progress has been achieved by the Sofia research group. This research has been extensively documented in a series of papers which were summarized by Denkov and coworkers (7a and b). One of the early debates was concerned with the question of whether the antifoam globules primarily cause rupture of the individual foam films or, alternatively, become expelled from the thin films and later become trapped in the adjacent PBs. In the case of the trapped globules, the shrinking of the PB to dimensions comparable to that of the drop size would ultimately force the droplet to enter the air/water surface, causing rupture which could be regarded as a secondary process. Interestingly, both mechanisms had been observed previously in different systems.

It was rightly anticipated that the kinetics and antifoam efficiencies differ for the two mechanisms; in the case of the globules directing entering and breaking the foam films, this action was considered as "fast antifoaming," as originally documented by Koczi and coworkers (9). These workers considered the role of the pseudo-emulsion film in the breaking of foam by using both hydrophobic particles and heterogeneous antifoamers (hydrophobic particles and oil). The direct rupture of the pseudo-emulsion film was again considered to be the primary step for heterogeneous (particle/oil) antifoaming, which eventually leads to a bridging mechanism and finally to rupture of the foam film, as indicated in Fig. 10.13.

However, as an alternative, if the antifoam globules first escape from the foam film into the PB, then this process can be regarded as a relatively slow antifoaming mechanism. Clarification of the mechanism is clearly of practical importance since it has been suggested that it may be possible to tailor the size distribution of the globules to fit the dimensions of the foam cross-sectional thickness of the lamellae or within the PB. Intensive experimental studies were carried out based on direct microscopic observations of the foams and foam films (including some of the foam destruction events) and by the implementation of a novel experimental technique involving trapping the films. From these fundamental studies, it was established that both mechanisms may occur depending on the particular systems.

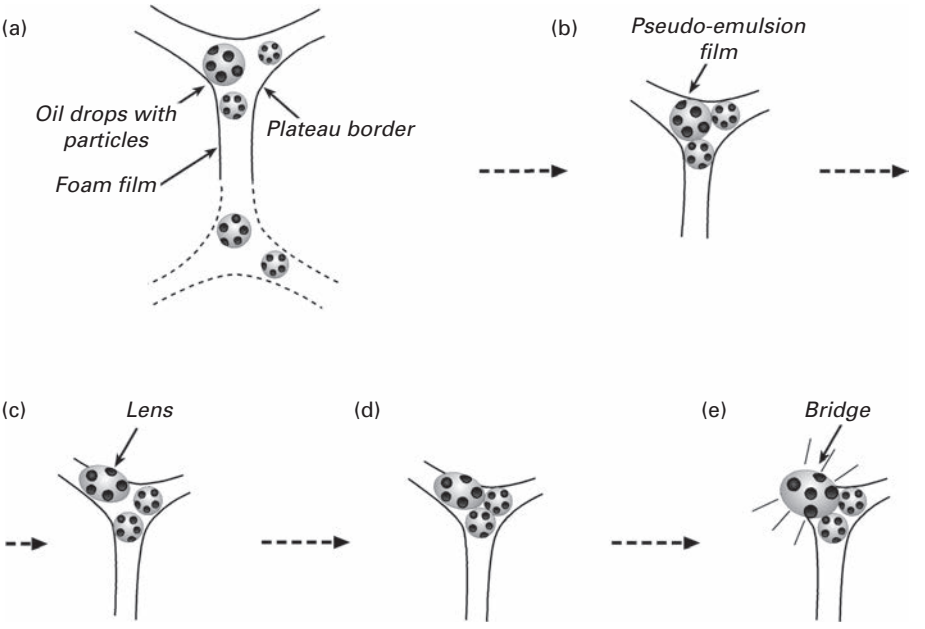

Fig. 10.13 The suggested antifoaming mechanism for a mixed-type antifoamer: (a) oil drops (containing solid particles) collect in the Plateau border; (b) the drops become trapped in the thinning border; (c) the pseudo-emulsion film breaks directly, and a drop enters and forms a solid plus oil lens; (d) the lens becomes trapped during thinning; (e) the lens bridges the film at the plateau border and the bridge. From ref (9a).

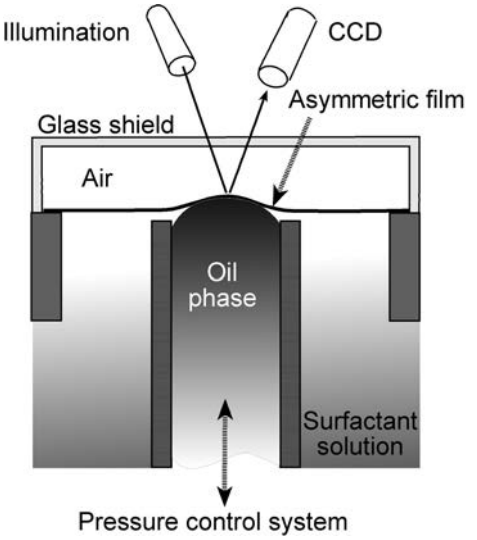

Fig. 10.14 Set-up for observation of asymmetrical oil/water/air film. Formed by pressing a compound under the solution surface. From ref (31).

Denkov and coworkers (31, 32) developed a thin film apparatus (shown in Fig. 10.14) which enabled a series of experiments to be carried out with asymmetric films of millimeter size. A drop of oil is initially released from a capillary and allowed to float up on the action of buoyancy and eventually presses against the interface, thus establishing the film. The cell is covered by an optically clean glass, and the films were observed from above in reflected light by a microscope. Using this method, one can observe the process of film rupture by the droplet or particle which protrudes from the compound globule into the aqueous film. The film thickness at the point of rupture can also be measured. From microscopic observations of the mixed antifoam compounds (comprising silica oil and silica particles) it was found that hole formation in the foam film occurred during the early stages of the thinning process, causing rupture within seconds, and these data verified the fast mechanism of antifoaming.

A shaking test using similar mixed formulations also showed that breakage occurs rapidly (< 10 s), confirming the microscopic observations. In these studies, a bridging/stretching mechanism was proposed in which the antifoam globule connected the surface of foam film, producing an unstable oil bridge. The initial stretching was due to uncompensated capillary pressures at the oil/air and oil/water interface, which eventually ruptured the entire foam film. Further work showed that this fast mechanism was the characteristic for several mixed oil silica antifoams with both ionic- and nonionic-type surfactants. However, in the case of pure oil (without silica particles), similar experimental methods indicated the antifoaming action occurred through the oil droplets flowing from the foam films (without rupture) during the thinning and gradually accumulating in the PBs. During the thinning of the PBs, the trapped oil drops are compressed in the film, and as the compression forces increase, longer time scales (several minutes) were involved in the rupture process. This can be considered as a "slow antifoam action" and has been observed in many practical systems.

The slow antifoam action can be illustrated for foams generated by circulating liquid through a glass cylindrical column as shown in Fig. 10.15(a), (b) and (c) where the drops are shown to become expelled from the foam film into the PBs and compressed, forming asymmetric oil/water/air films. In Fig. 10.15(d), the foam decay process is documented in terms of the change in foam height versus time. Through drainage the initial decay process begins to occur (I) followed by a stabilizing step in which the drops flow into the PBs (II) but on compression the film eventually breaks causing instability (III) leading to the residual (IV). During this compression step, it is the magnitude of the capillary pressure which determines the point of rupture, and this must exceed a critical value for the oil drops to enter the walls.

From additional experimental studies carried out using a new type of cell, it was found that the most important parameter that decided whether the oil globule enters directly into the foam film or acts by flowing into the Plateau borders was the magnitude of the entry barrier E_c. This value was used as the criteria for the transition process and defines the time scale of the defoaming action.

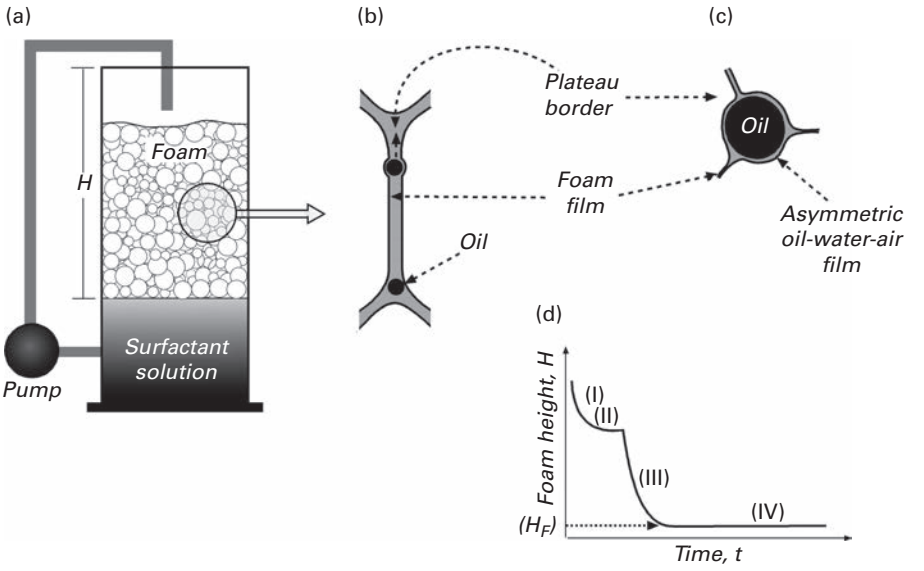

Fig. 10.15 The steps are assigned as (I) initially drainage occurs and the globules flow into the PB where some degree of stability is achieved and (II) eventually the compression pressure is sufficient to break the film causing instability (III) until finally a residual low foam volume state is reached in step (IV). From ref (31).

10.13 Critical entry pressure for foam film rupture

The thin film trapping technique (FTT) developed by the Sofia research group is illustrated in Fig. 10.16. A glass cell containing the aqueous surfactant solution and the dispersed antifoam oil droplets rests on a flat microscopic stage. Initially, a glass vertical capillary tube, which is enclosed in the cell, is gradually lowered into a chamber and submerged below the solution, and the air pressure P_A inside the capillary (which is externally controlled and monitored) is then increased. This causes the convex air/water meniscus in the capillary to press against the glass substrate, forming a wet film (glass/water/air) in which the antifoam globule is then trapped and compressed (as indicated in Fig. 10.16(b)). This compression process is observed by an optical microscope positioned below the stage. Eventually, the trapped antifoam globules enter (pierce) the surface of the wetting film at a critical capillary pressure. This value corresponds to the point of rupture and the pressure of the air/water meniscus around the trapped drops $P_C = P_A - P_W$, where P_W is the pressure in the aqueous film. Further observation showed that, following rupture of the film, the oil enters the air/water interface where it either spreads or forms a lens. The critical air/water capillary pressure for rupture of a thin asymmetric film of water separating air from an oil droplet could be measured and, from these results, the entry barrier of actual micrometer-sized antifoam globules could be calculated. Experiments were carried out with a range of different formulations and it was found that higher entry

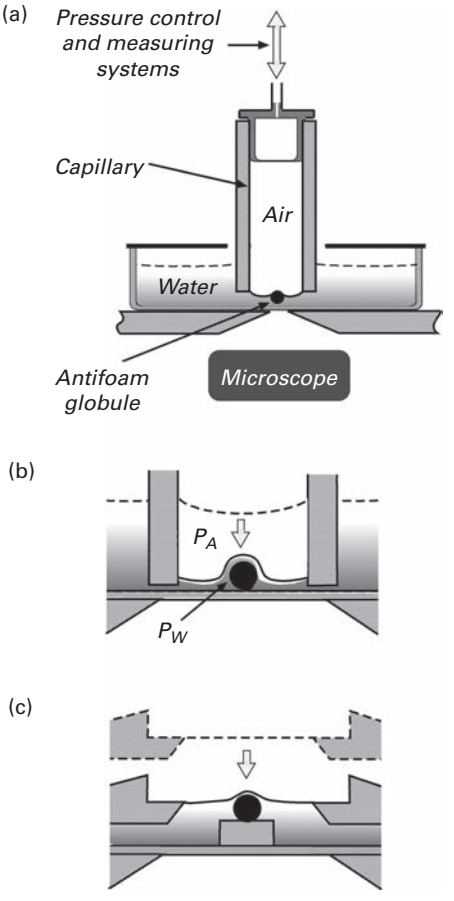

Fig. 10.16 The experimental setup of the FTT: (a) Vertical capillary, partially immersed in surfactant solution containing antifoam globules, is held close to the bottom of the experimental vessel. (b) The air pressure inside the capillary, P_A, is increased and the convex air/water meniscus in the capillary is pressed against the glass substrate. Some of the antifoam globules remain trapped in the formed glass/water/air film and are compressed by the meniscus. At a given critical capillary pressure ($= P_A - P_w$), the asymmetric film formed between the antifoam globule and the solution surface ruptures and an event of globule entry is observed by an optical microscope. (c) Another modification called "gentle FTT" is used for measuring low-entry barriers – an initially flat meniscus is formed, which allows the trapping of antifoam globules at a virtually zero capillary pressure. From ref (31).

barriers prevented or reduced the chances of the drop entering the film. In the case of systems with low entry barriers where an initially flat meniscus was formed, the equipment was later modified to enable more precise measurements.

Extensive measurements using several different types of oils, compounds and surfactants (32) and drops of different sizes with different concentrations of solid particles in the compound were carried out. The data were collected and presented as a graph, relating the foam lifetime to the entry barrier as shown in Fig. 10.17. In this graph two

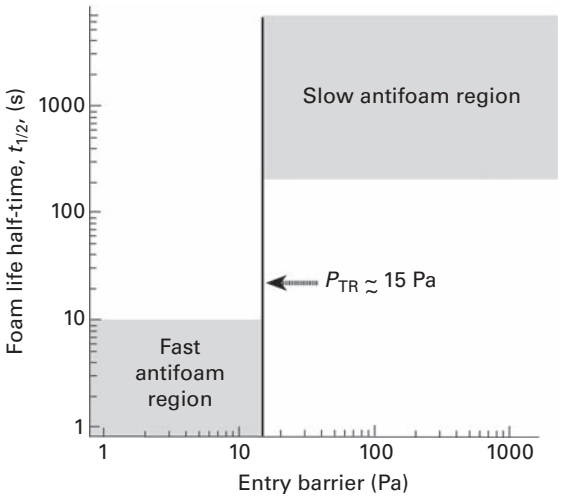

Fig. 10.17 The entry barrier versus foam stability (lifetime) measured for many different types of surfactant/antifoam systems: The experimental data were found to fall into two distinct regions: systems in which the foam is destroyed in less than 5 s (fast antifoams) and < 15 *P*a and systems for which the defoaming time is longer than 8 min (slow antifoams) and > 20 *P*a. From ref (32).

well-defined distinct regions were obtained which were separated by a threshold value corresponding to a transition value of $P_{TR} \approx 15$. This critical value of could be used to distinguish the fast (foam film breaking) from the slow (PB breaking) antifoams. In the fast defoaming region, generally $P_{TR} < 15$, and the process occurred in less than 10 s, but in slow defoaming with $P_{TR} > 15$, a longer time period was needed (> 5 min).

From these studies it was reported that the hydrophobic solid particles could also have the effect of reducing the entry barrier by one to two orders of magnitude. However, in some cases the entry barrier remained higher than the threshold value, P_{TR}, and the compound was unable to break the foam films, resulting in the globules being expelled from PBs during thinning of the film, as earlier discussed. From microscopic observations, it was also shown that the oil bridge, once formed, was subject to stretching until its thickness was reduced at a local point where it finally ruptured. This stretching /bridging mechanism is different from the bridging by a rigid, solid particle where the foam film breaks by dewetting. The bridging theory of an oil drop was also extended to include this concept of non-uniform film thickness in the immediate vicinity of the drop even when the bridge was initially formed. Although the same instability criteria $B_c > 0$ were used, modifications were made to include the stretching concept.

10.14 Influence of the hydrophobicity of solid particles on E_c

The influence of the degree of hydrophobicity of the particles on the efficiency of the defoaming action was also investigated by the Sofia research group. Experiments were carried out by mixing hydrophilic silica particles with silicone oil at room temperature

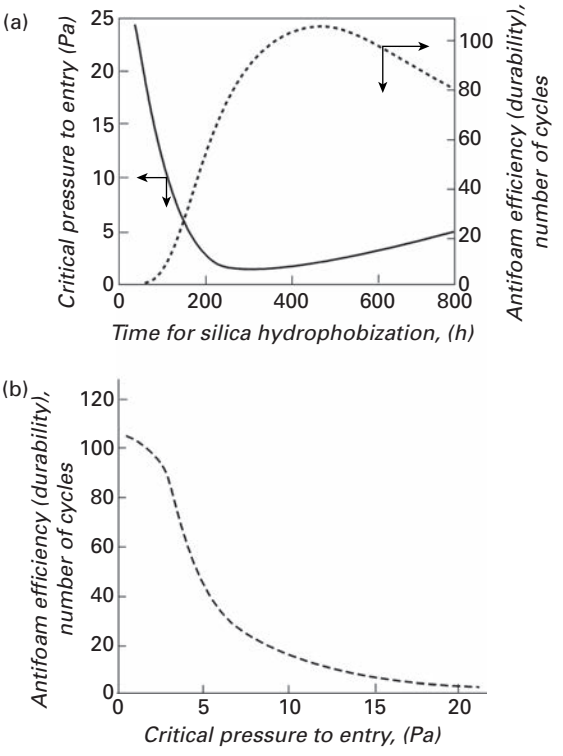

Fig. 10.18 (a) Critical pressure for globule entry and antifoam efficiency of a silicone oil–silica compound in 10 mM AOT solution, as functions of the time of silica hydrophobization. (b) The dependence of the compound efficiency on solutions of three different surfactants: 10 mM anionic AOT, 0.6 mM nonionic APG, and 1 mM nonionic Triton X-100. From ref (7).

and storing the mixture with mild stirring for a long time period. This caused silicone oil to gradually adsorb on the surface of silica particles, but several weeks were required to reach a high degree of hydrophobicity. Based on this procedure, particles with a wide range of surface hydrophobicities were prepared. The antifoam efficiency of each of these systems was then evaluated (32c) using an automatic shake test in which foams were generated from a surfactant solution containing low levels of the antifoaming compound (0.01%). In the shaking tests, agitation was carried out as a series of consecutive shake cycles (each cycle of agitation was 10 s), and the defoaming time was quantified (which was defined as the time for appearance of a clean water/air interface without bubbles) after each cycle. The antifoam efficiency was tested every day and recorded in terms of the number of cycles required to exhaust the compounds. Fig. 10.18(a) shows a plot of the relationship between the critical pressure of entry P_A determined from the FTT, the antifoam efficiency as evaluated in terms of the number of cycles and the hydrophobicity of the silica particles (determined from the hydrophobization time). These data were also expressed in Fig. 10.18(b) in which a well-pronounced maximum can be seen corresponding to a hydrophobization time of about 300 hours, a low critical pressure of entry of two and an antifoaming efficiency of five shaking cycles.

The presence of the maximum was discussed in terms of the balance between the hydrophobicity of the particles, which is defined by a critical degree of dewetting at the oil/water and air/water interfaces (which is required to destabilize the asymmetric oil/water/air films). To summarize, an active antifoamer (with a low entry barrier) was considered to require an optimal hydrophobicity to balance these two requirements. In Fig.10.18(b), the relationship between the antifoam efficiency and the magnitude of the entry barrier is shown for the systems studied and indicates a correlation between the decrease in antifoam efficiency and the increase in entry pressure. For spherical particles, the optimal hydrophobicity was expressed as a most favorable three-phase contact angle solid/water/oil (31).

10.15 Influence of the pre-spread oil layer on E_c

From FTT it was shown that the presence of a pre-spread oil layer at the air/water interface can also change E_c and facilitate or hinder the entry of drops. From the experiments, the effect of oil spreading on the entry barrier was quantified and the results showed that E_c was reduced by several times the entry barrier for mixed oil/silica compounds. It was also found (31) that the entry barrier in many systems is below the threshold value $P_{TR} \approx 15\ P_A$, but only in the presence of a pre-spread layer of oil. It could be proposed that these antifoams behave as fast ones only because the oil spreads rapidly on the solution surface during foaming, reducing in this way the entry barrier below P_{TR}. The results for the entry barrier of oil drops (without silica) also showed a moderate reduction of the entry barrier by pre-spread oil in most systems (32).

10.16 Ageing effects with chemical antifoamers

Antifoams are usually very active when initially added to a foam system but usually age or become exhausted after a certain period of time. There are many reasons for this deterioration in performance, and it is a general occurrence in many different types of antifoam. Some of the explanations are outlined in Fig. 10.19.

For example, decomposition due to chemical oxidation of a fatty acid containing unsaturated groups, or the hydrolysis of certain silicones under acidic or basic conditions, may occur with time. This could lead to changes in the surface tension of the materials, thus causing differences in the entering, spreading and bridging characteristics of the antifoamer. In addition, the size of the antifoaming droplet may change. Droplets may become emulsified under shear, and when the size falls below 5 μm, thermal energy will dominate over gravity. There is also the possibility that the smaller globules which remain in solution will no longer be buoyant and capable of entering the air/water interface. By predicting the balance between the buoyancy forces and the thermal forces, Bergeron (33) derived an equation for the critical radius, which corresponded to the optimum antifoamer performance. Drop size may be changed by

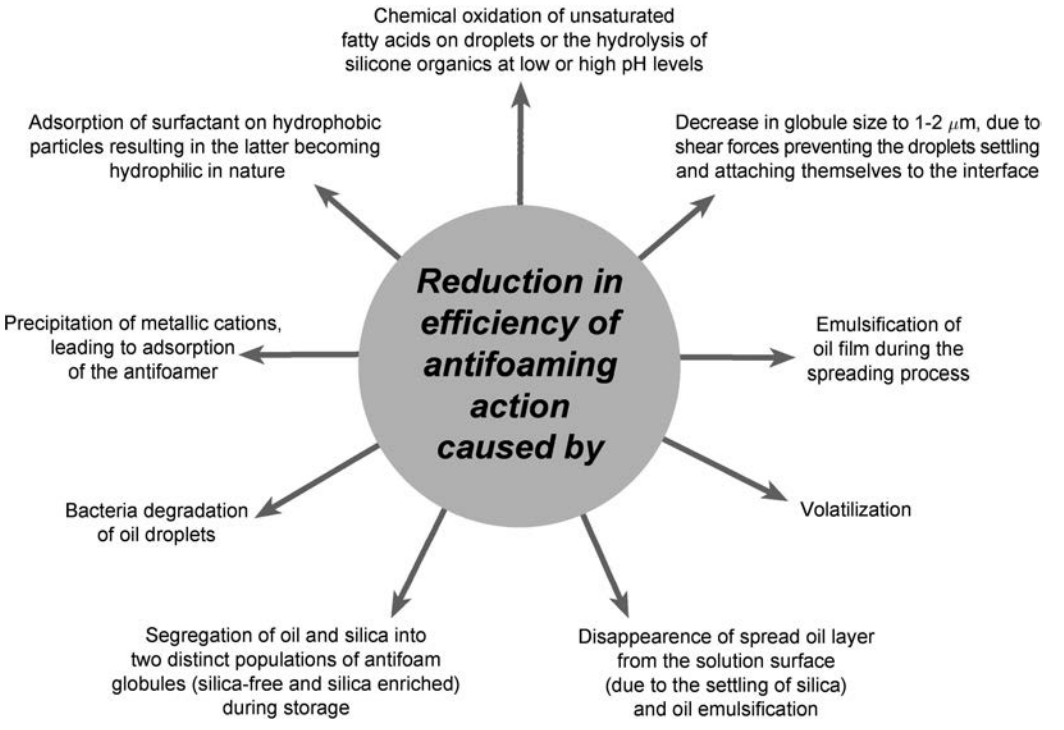

Fig. 10.19 Some of the aging effects of antifoamers.

modifying the drop viscosity and the interfacial tension. Frequently, the formulation can be reactivated by adding fresh oil.

Denkov and coworkers (32) have experiments on the exhaustion and reactivation of antifoam mixtures with a foaming system containing an anionic surfactant (sodium dioctylsulfosuccinate) and silica. Shaking tests were used to evaluate the time of destruction (breakage time) since this is a simple measure of the antifoam efficiency, but aging effects also can be evaluated by repeating the shaking tests using a cyclic procedure to see if the antifoam can function over repeated operations. The results indicated that the time for foam destruction increased with each cycle, confirming the deterioration in performance. For the initial cycles, only about 5 to 10 secs were required for foam destruction, but after 45 cycles, 60 secs were needed to break the foam, indicating it was approaching exhaustion. Further experiments showed that by adding a portion of oil (without particles) it was possible to restore the performance, but on continuously repeating the cycle destruction occurred. This situation is illustrated in Fig. 10.20, where a consecutive series of exhaustion/reactivation cycles are shown. This restoration process was found to occur even when the oil was only a weak antifoamer.

To explain the exhaustion of mixed silica/silicone oil antifoams, it was necessary to consider two closely interrelated processes. Initially, the partial segregation of the silica from the oil resulted in two separate fractions: globules consisting of silica free and

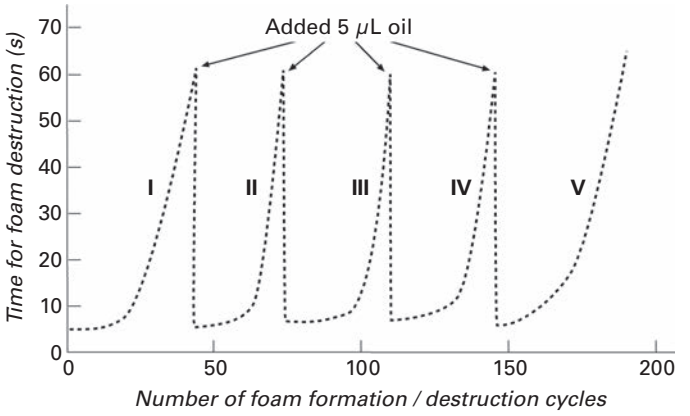

Fig. 10.20 Consecutive cycles of exhaustion and reactivation of mixed oil/silica compound in 10 mM solution of the anionic surfactant sodium dioctyl-sulfosuccinate (AOT). An initially active antifoam (defoaming time ≈ 5 s) gradually loses its activity with the number of foam formation/destruction cycles in a standard shake test. The introduction of silicone oil results in a perfect restoration of the antifoam activity. Five exhaustion curves (indicated by roman numbers; the symbols indicate the experimentally measured defoaming time) and the corresponding four reactivation events (the vertical dashed lines) are shown. From ref (32c).

silica-enriched oil fractions. Both these separate population were considered as less active defoamers since silica-free particles were unable to enter the air/water interface and destroy the lamellar. The entry barrier was too high and also the silica-enriched globules caused a deficiency in oil in the system which prevented the spread of oil layer on the interface. In addition, the spread oil layer was used up by emulsification as the foam films ruptured. These processes gradually caused the system to become exhausted but reactivation was achieved. Fresh additions of PMS caused a new spreading of the oil layer and a rearrangement of particles in the oil droplets. This produced a fresh antifoam system. The sequence of events is shown in Fig. 10.21.

With the use of the mixed defoamers, it is essential to keep the two components together to ensure synergism, particularly in laundry, pulp processing, etc., which involves repeated agitation action.

10.17 Physical methods of defoaming

The use of "foam breaking chemicals" or inhibitors may contaminate some products such as food, bioprocesses used for paper and drug production and the synthesis of antibiotics. Unwanted foaming can also occur during water purification, blood transfusions and dyeing of fabrics, and the use of chemical antifoamers is usually avoided. In fact, in many bioprocesses there is little detailed knowledge of the impact of chemical antifoamers on the cells or product. In some cases, certain concentrations of antifoams appear to have a detrimental effect upon cells and protein production, and the effects vary depending upon the protein (34). To avoid

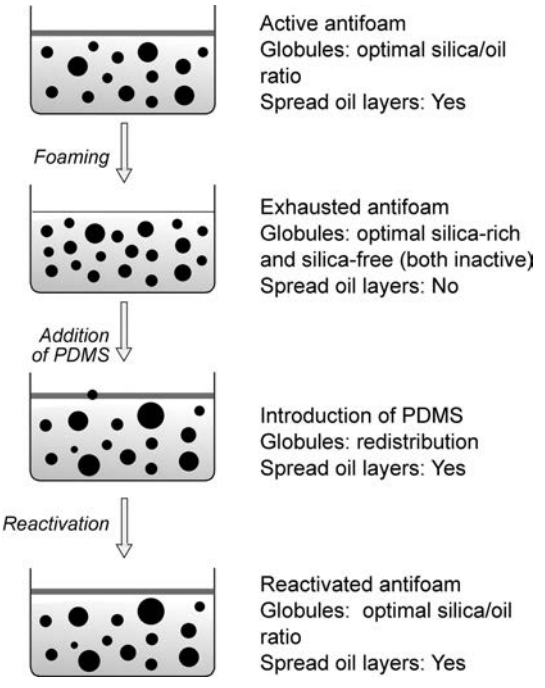

Fig. 10.21 Schematic presentation of the processes of antifoam exhaustion and reactivation of emulsified oil–silica antifoam compound. From ref (32).

this problem, physical methods of foam control have been developed based on mechanical methods such as spraying, projecting air-streams, horizontal rotating discs fitted to the top of bubble columns, spinning blades, turbines, paddle wheels, forcing foam through a wire stream, heat (hot wires above the rising foam), sparks, etc. The use of the orifice defoamers method has been discussed by Garrett (2). Some of these techniques have proved to be fairly effective in destroying foams. Another possible solution to this problem is to use weak ultrasonic shock waves above the surface of the foam and this has proved fairly successful in recent years, especially since the development of the piezoelectric transducers. Winterburn and Martin (35) earlier established that placing the ultrasonic generator in the aqueous phase was ineffective.

10.17.1 Ultrasonics

The exact mechanism by which foam is destroyed by ultrasonic vibration is still not clear, although several explanations have been put forward. Essentially, it is important to consider the fact that velocity of sound is lower in foam than in air or water, and the wavelength of the sound wave decreases as it passes into foam from air. Sound is also attenuated when passing through foam. Early work by Sandors and Stein (36) suggested that the defoaming action involved the process of marginal regeneration and squeezing of surface waves along the film and PB boundaries and causing thickness

fluctuations. This may cause faster local drainage, leading to bubble coalescence and breaking. Garrett (2) suggested that in some cases, the defoaming by ultrasound possibly involved a resonance of the mesostructures of the foam. It was shown that ultrasonic vibrations can both prevent the formation of foams and destroy foams stabilized with sodium dodecyl sulfate surfactant, and vibrators with higher power consumption are more effective. Alternative suggestions such as the effect of unidirectional radiation pressures and induced resonant vibrations in the bubbles have been discussed.

There are in the literature several industrial patents describing the application of low-frequency vibrations (20–20000 Hz) to destroy certain types of detergent foams. Ultrasonic vibrations have also been used for foam control during fermentation, pumping of jet fuel oil, degassing, etc. Sun (37) destroyed very tough foams in flotation cells using a high-power air-driven siren. Dorsey (38) used air-driven ultrasonic generator to control foam during fermentation. Morey and coworkers (39) found high-intensity ultrasonic vibrations are effective at controlling dynamic foams and reported studies on both continuous foaming or static foams and the effect of gas flow rate and amplitude. In addition, a considerable amount of success has been achieved in breaking low-viscosity foams produced in the textile and dairy industries. In the brewing industry, to the author's knowledge, there is no ideal foam control method currently in use, although ultrasonics have been shown to suppress foaming in fermenting vessels. The ultrasound generated by ceramic piezoelectric transducers has unusual property that when an electric voltage is applied across their crystalline ceramic structure, deformation occurs with an alternating current which produces sinusoidal vibrations. The resonance frequency depends on the physical dimensions of the transducer and its surroundings. By using such a system, it is possible to focus the ultrasonic power on to a small volume of the surface foam.

Work on ultrasound in the area of control foam was carried out at the Guinness Brewing Worldwide Pilot Brewery in London (40). It was found that the older foams at the top of the foam layers are more susceptible to breakage with ultrasound, and there was also an effect over the entire foam surface. This was explained by reflection around the head-space of the vessel where the ultrasound can be reflected off the vessel walls and the liquid surfaces. The equipment is shown in Fig. 10.22, together with the schematics of the ultrasonic fields from the radiation plate and the influence of the position of the foam on the effectiveness of the breakage. It was shown that a wide beam of ultrasonic radiation was less effective than a focused beam.

Ultrasonic experiments by Dedhia and coworkers (41) related foam breaking to the and the ratio of the diameter of the horn to the column diameter of the horn and also to. Experiments were carried out in an acrylic column with an ultrasonic head operating at 20 kHz as an ultrasonic source with the tip of the horn above the foam. Foam was generated in the base of the column through a sintered glass sparger, and a surfactant solution of sodium lauryl sulfate was used in the column at a concentration below the CMC. The effect of the positioning of the horn on the foam collapse rate and also

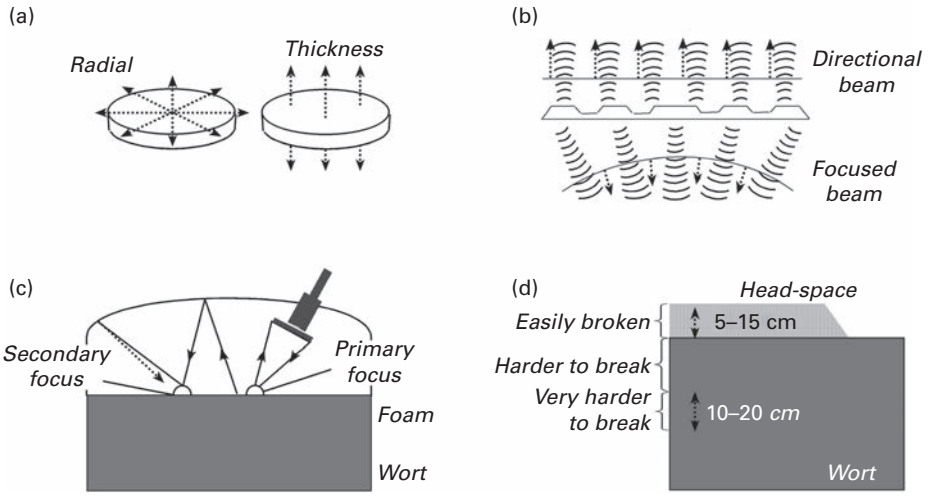

Fig. 10.22 Ultrasonic foam breaking: (a) equipment; (b) ultrasonic fields from the radiation plate; (c) effect of reflection around the vessel head-space; (d) the effect of foam position on ultrasonic foam breakage. From ref (40).

the effect of the pulse vibration using two horns of different diameter with a constant gas flow rate were studied. Efficiency of the ultrasonic horn was related to the position of the tip of the horn. The results of the study are summarized in Fig. 10. 23.

It was concluded from this study that the larger the diameter of the horn, the higher the foam collapse rate, and in addition, the column diameter plays an important role. An empirical equation correlating the initial foam collapse rate in the presence of an ultrasonic horn has been developed in terms of the initial liquid hold-up, surface tension of the surfactant solution and the ratio of the horn diameter to the column diameter.

In 2015, Garrett (2) summarized recent progress in ultrasound defoaming and provided some new insights into the mechanism. The process was described in terms of the delivery of acoustic energy, and the intensity was shown to be proportionate to the pressure fluctuations, which was partially transmitted and partly reflected from the foam surface. The acoustic transmission was highest for high gas volume fraction foams and lower for wet foams. Komarov and coworkers (42) used low frequency sound on foam stabilized by a water/glycerine mixture. In this study the existence of a critical threshold acoustic intensity (as measured by acoustic pressure) was established; an increase in frequency increased the threshold value, while an increase in viscosity decreased the value. Rodriguez and coworkers (43) studied the effect of ultrasonic intensity on a foamed soap solution at a frequency of 25.8 kHz and also found a threshold acoustic intensity below which foaming did not occur. Beyond the threshold, foaming increased with increase in the amount of energy and the time of application. Gas volumes and bubble sizes were also measured and the wavelength of the ultrasound calculated from the frequency and velocity of sound as a function of gas volume.

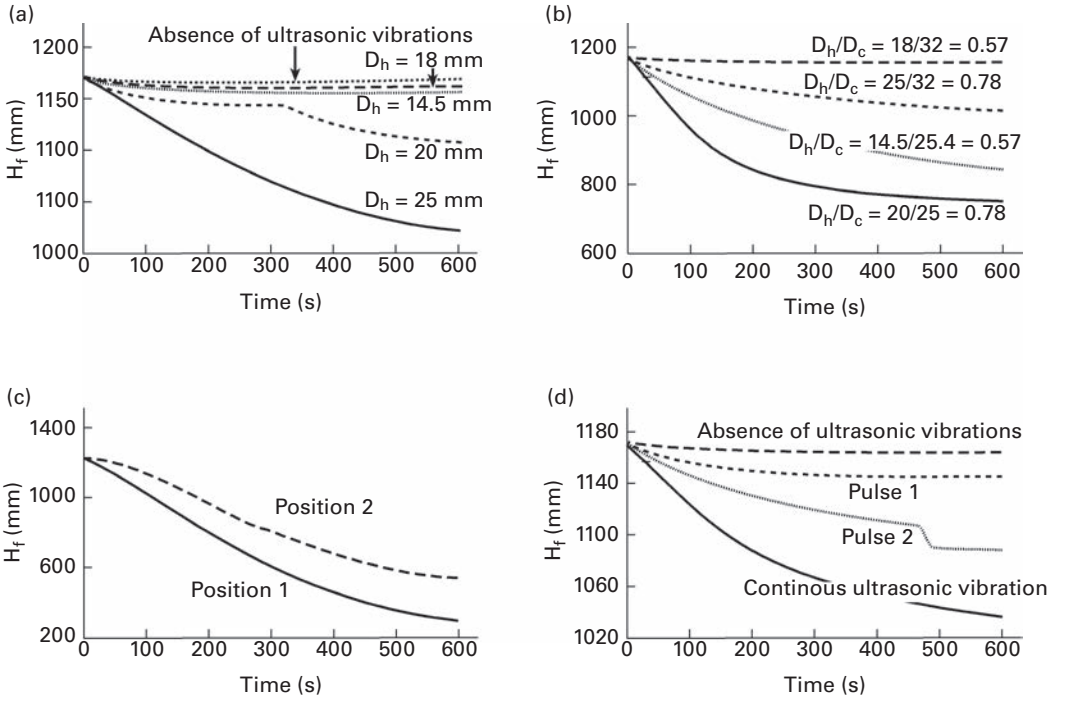

Fig. 10.23 (a) Effect of horn diameter (D_h) on foam collapse (column diameter (D_c) = 32 mm); (b) effect of collapse rate on the ratio of horn diameter to column diameter (D_h/D_c); data obtained from two different columns shows the same ratio does not give the same collapse rate (c) effect of position of the ultrasonic horn on foam collapse rate D_c = 23.4 mm. Position 1: Horn tip just touching the surface of the foam. Position 2: Horn tip 50 mm above the surface of the foam. (d) Effect of pulse vibrations on foam collapse. Horn diameter D_h = 25 mm, D_c = 32 mm. From ref (41).

Ben Salem and coworkers (44) in 2015 built up a more fundamental structure of the ultrasonic break-down process from studies carried out at constant frequency, with acoustic intensities below the threshold for defoaming. The change in amplitude of the ultrasonic signal of constant incident intensity across a foam sample of known thickness was used as a measure of the attenuation of the intensity. The phase differences gave the transit time across the foam and the speed of the sound. The relative amplitude was found to vary as a function of time as the bubble size increased due to diffusion disproportionation and the relative amplitude was plotted against time. This gave a pronounced minimum at a transitional time, indicating a maximum in the rate of energy adsorbed by the foam. The data also enabled a critical bubble size to be evaluated from a plot of evolution of bubble size versus time, and a comparison of the transitional times and critical bubble sizes for different types of foam systems with critical bubble sizes (in the same range) was made. This enabled these workers to suggest that at the critical radius the bubble becomes resonant and pumps a maximum energy from the incident signal, which led Garrett (2) to suggest that the critical bubble radius would probably be a function of the acoustic frequency. Defoaming becomes maximal if the bubble size corresponds to the critical

size range for the resonance frequency; by increasing the intensity of that frequency, more effective defoaming occurs. However, Garrett (2) noted that increasing the frequency above the resonant frequency for a foam of given bubble size will lead to less efficient energy-level transfer into the foam, which would therefore need higher threshold acoustic intensities for defoaming, as demonstrated by Komarov (42). To achieve maximum defoaming efficiency, multiple frequency generators would be required that need be optimized according to the bubble size distribution in polydispersed foam systems

10.17.2 Suppression of foam by the adjustment of the vessel wettability

Foam control can be achieved by adjusting the size of the vessel and wettability of the side walls of vessels. Cheah and Cilliers (45) showed that the amount of foam generated from the anionic surfactant, sodium bis-2 (ethylhexyl) sulfosuccinate (AOT) by the plunging jet method decreases for larger vessels. This dependence on container size was verified by Papara and coworkers (46), who also showed that the wettability of the sidewalls of the vessel is also another important factor to consider. In their experiments, foams were generated from a mixture of soya protein isolate and xantham gum using a kitchen mixer in plexiglass containers that they termed "hydrophobic" (water contact angle (θ) ~ 98–112°) or "hydrophilic" (θ ~ 75°) and they observed higher drainage rates in small, hydrophilic vessels. However, in hydrophobic vessels, the drainage rates were found to be similar between the small and medium-sized vessels. In fact, the large vessel exhibited the fastest drainage rates independent of the hydrophobicity of the container. Zuidberg (47) has also shown that the wettability of solid surfaces is important in bubble formation at the liquid/solid interface by studying bubble formation in beer.

More recently, Hamlett and coworkers (48) showed that changing the wettability of the inside surface of glass vessels by chemical treatments using silanes was an effective method of suppressing foamability. The foaming properties of aqueous solutions of a nonionic surfactant (hepta-ethylene glycol monododecylether, $C_{12}E_7$), an anionic surfactant (sodium dodecyl sulfate) and a cationic surfactant (hexadecyltrimethylammonium bromide) in glass vials of different wettabilities were measured. The concentrations of the surfactants were above the CMC. It was found that highly hydrophobic vials ($\theta > 90°$) suppress the foam formation and that this effect was independent of surfactant type. However, the surfactant type seems to be important when considering foam stability because the stability of the anionic surfactant (SDS) foam was influenced by hydrophobic surfaces to a much greater extent than the cationic (CTAB) and nonionic ($C_{12}E_7$) surfactants. The study was extended to investigate the effect of the wettability of the containers on the foam stability of four different beers. The hydrophobic glasses into which the beers were poured suppressed both the formation of the beer head and the stability of the bubbles for several different types of beers. In Fig. 10.24, the influence of the hydrophilic/hydrophobic nature of the glass wall (50/50) on the bubble size of a beer is shown.

Fig. 10.24 The effect on beer foam and bubble formation at the beer/glass interface in a glass exhibiting both hydrophilic and hydrophobic surfaces. From ref (48).

In addition, the bubble structure of champagne was also found to be influenced by the hydrophobicity of the glass vessel. This method may also be useful for foam control in such processes as the bottling of beverages and fruit juices.

References

(1) P. R. Garrett, Ed., *Defoaming: Theory and Industrial Applications*, Marcel Dekker, New York, 1993.
(2) P. R. Garrett, Defoaming: Antifoams and Mechanical Methods, *Curr. Opin. Colloid Interface Sci.*, **20**, 81–91, 2015.
(3) M. J. Owen, *Defoamers, Encyclopedia of Chemical Technology, Kirk-Othmer*, Wiley and Sons Ltd., Hokboken, New Jersey, USA, 2000.
(4) H. T. Kerner, *Foam Control Agents*, Noyes Data Corp., New York, 1976.
(5) R. J. Pugh, *Foam Breaking in Aqueous Systems, Chapt 8, Handbook of Applied Surface and Colloid Chemistry*, Ed. K. Holmberg, Wiley & Sons, Ltd, Hokboken, New Jersey, USA, 2001.
(6) R. Bagwe, Phosponium Ionic Liquid as Defoamers; Structure–Property–Application performance Correlation, Abstract 13th ICSCS/83rd CSS Symposium, June 14–19, New York, 2009.
(7a) N. D. Denkov, Mechanism of Foam Destruction by Oil Based Antifoams, *Langmuir*, **20**, 9463–9505, 2004; (b) N. D. Denkov, P. Cooper and J. K. Martin, Mechanism of Action of Mixed Solid/Liquid Antifoamers 1. Dynamics of Foam Film Rupture, *Langmuir*, **15**, 8514–8529, 1999.

(8) Lobo, A. D. Nikolov and D. T. Wasan, Foam Stability in the Presence of Oil, *J. Disp. Sci. Technology*, **10**, 143–159, 1989.
(9a) K. Koczo, J. K. Kozone and D. T. Wasan, T., Mechanism of Antifoaming Action in Aqueous Solutions by Hydrophobic Particles and Insoluble Liquids, *J. Colloid Interface Sci.*, **166**, 225–238, 1994; (b) D. T. Wasan, K. Koczo and A. D. Nikolov, Mechanism of Aqueous Foam Stability and Antifoaming Action with and without Oils; A Thin Film Approach, in Foams, Fundamentals and Applications in the Petroleum Industry, *Advances in Chemistry Series*, No. 242; L. L. Schramm (Ed.), *American Chemical Society*, Washington, DC, pp. 47–114, 1994.
(10) V. Bergeron, M. E. Fagan and C. J. Radke, Generalized Entering Coefficients: A Criteria for Foam Stability, *Langmuir* **9**, 1704–1713, 1993.
(11) F. Gao, K. Van, Q. Wang and S. Yuan, Mechanism of Foam Destruction by Antifoams: A Molecular Dynamic Study, *Phys. Chem. Chem. Phys.*, **10**,17331–17337, 2014.
(12) X. Shu and Coworkers, pH Responsive Aqueous Foams of Oleic Acid/Oleate Solutions. *J. Dispersion Sci. Technol.*, **35**, 293–300, 2014.
(13) R. J. Pugh, The Role of the Solution Chemistry of Oleic Acid and Dodecylamine in the Flotation of Calcium Fluoride, *Colloids Surf.*, **18**, 19–41, 1986.
(14) H. Zhang, C. A. Miller, P. R. Garrett and K. H. Raney, Mechanism for Defoaming, by Oils and Calcium Soap in Aqueous Systems, *J. Colloid Interface Sci.*, **263**, 633–644, 2003.
(15) J. Venzer and S. P. Wilkowski, Trisiloxane Surfactants – Mechanism of Spreading and Wetting. In *Pesticide Formulations and Applications Systems*, Vol. **18**, ASTM Special Technical Publication, STP 1347, American Society for Testing and Materials, West Conshohocken, PA, pp. 140–151, 1998.
(16) B. K. Jha, A. Patist and D. O. Shah, Effect of Antifoamer on the Micellar Stability and Foamability of SDS Solution, *Langmuir*, **15**, 3042–3044, 1999.
(17) I. Blute, M. Jansson, S. G. Oh and D. O. Shah, The Molecular Mechanism for Destabilization of Foams by Organic Ions, *J. Amer. Oil Chem. Soc.*, **71**, 41–46, 1994.
(18) P. R. Garrett, The Mode of Action of Antifoams, in Defoaming. In *Surfactant Science Series*, Ed. P. R. Garett., Vol. **45**, Chapter 1, Marcel Dekker, New York, pp. 1–118, 1993.
(19) G. Johansson and R. J. Pugh, The Influence of Particle Size and Hydrophobicity on the Stability of Mineralized Froths, *Int. J. Miner. Process.*, **34**, 1–22, 1992.
(20) A. Dippennar, The Destruction of Froths by Solids, 1, *Int. J. Miner. Process.*, **9** (1), 1–14, 1982.
(21) A. Dippennar, The Destruction of Froths by Solids, 2. The Rate Determining Step, *Int. J. Miner. Process.*, **9**, 15–22, 1982.
(22) G. D. M. Morris, J. J. Cilliers and S. Neethling, The Effect of Hydrophobicity and Orientation on Cubic Particles on the Stability of Thin Film, *Miner. Eng*, **23**, 979–84, 2010; G. D. M. Morris, J. J. Cilliers and S. Neethling, A Model for Investigating the Behaviour of Non-Spherical Particles at Interfaces, *J. Colloid Interface Sci.*, **354**, 380–385, 2011; G. D. M. Morris and J. J. Cilliers, Behaviour of a Thin Film Revisited, Dippennar, *Int. J. Miner. Process.*, **131**, 1–6, 2014; G. D. M. Morris, J. J. Cilliers and S. Neethling, An Investigation of the Stable Orientation of Orthorhombic Particles in Thin Films and Their Effect on Its Critical Failure Pressure, *J. Colloid Interface Sci.*, **361**, 370–380, 2011.

(23) K. Brake, The Surface Evolver, *Experimental Maths*, **1** (2), 141–165, 1992.
(24) G. C. Frye and J. C. Berg, Mechanism of the Synergistic Antifoam Action of Hydrophobic Solid Particles in Insoluble Liquids, *J. Colloid Interface Sci.*, **130**, 54, 1989.
(25) K. Vijayaraghavan, A. Nikolov and D. Wasan, Foam Formation and Mitigation in Three-Phase Gas-Liquid-Particulate System, *Adv. Colloid Interface Sci.*, **123**, 49–61, 2006.
(26) K. S. Joshi, S. A. K. Keelani, C. Blickenstorfer, I. Naegeli. C. Oliviero and E. J. Windhab, Nonionic Block Copolymers, *Langmuir*, **22**, 6893–6904, 2006.
(27a) K. S. Joshi, S. A. K. Keelani, C. Blickenstorfer, I. Naegeli, E. J. Windhab, Influence of Fatty Alcohol Antifoamers on Foam Stability, *Colloids Surf., A*, **263**, 239–249, 2005; (b) K. S. Joshi, A. Baumann S. A. K. Jeelani C. Blickenstorfer, I. Naegeli and E. J. Windhab, Mechanism of Bubble Coalescence Induced by Surfactant Covered Antifoam Particles, *J. Colloid Interface Sci.*, **339**, 446–453, 2009.
(28) H. Zhang, C. A. Miller, P. R. Garrett and K. H. Raney, Defoaming Effect of Calcium Soap, *J. Colloid Interface Sci.*, **279**, 539–547, 2004.
(29) L. Ran, Characterization, Modification and Mathematical Modelling of Sudsing, *Colloids Surf., A*, **382**, 50–57, 2001.
(30) P. R. Garrett, S. P. Wicks and E. Fowles, The Effect of High Volume Fractions of Latex Particles on Foaming and Antifoaming Action in Surfactant Solutions, *Colloids Surf., A*, **263**, 282–283, 307–328, 2006.
(31) K. Marinova and N. D. Denkov, Foam Destruction by Mixed Solid/Liquid Antifoams in Solution of Alkyl Glucoside, Electrostatic Interactions and Dynamic Effects, *Langmuir*, **17**, 2426, 2001.
(32a) A. Hadjiiski and Coworkers, Gentle Film Trapping Technique with Application to Drop Entry Measurements, *Langmuir*, **18**, 127, 2002; (b) A. Hadjiiski and Coworkers., Role of Entry Barriers in the Foam Destruction by Oil Drops, *Proceedings of the 13th Symposium on Surfactants in Solution*, published in *Adsorption and Aggregation of Surfactants in Solution*, Ed. K. L. Mittal and D. Shah, Marcel Dekker, New York, Chapter 23, p. 465, 2002; (c) K. Marinova and Coworkers, Optimal Hydrophobicity of Silica in Mixed Oil–Silica Antifoams, *Langmuir*, **18**, 3399, 2002; (d) N. D. Denkov, S. Tcholakova, K. Marinova and A. Hadjiiski, Role of Oil Spreading for the Efficiency of Mixed Oil–Solid Antifoams, *Langmuir*, **18** (15), 5810–5817, 2002; (e) N. D. Denkov and K. Marinova, Antifoaming Action of Oils, *Proceedings of the 3rd Euro Conference on Foams, Emulsions and Applications*; (f) A. Hadjiiski, and Coworkers, Role of Entry Barriers in the Foam Destruction by Oil Drops, *Proceedings of the 13th Symposium on Surfactants in Solution*, Ed. K. L. Mittal, B. Moudgil and D. Shah, Marcel Dekker, New York; (f) A. Hadjiiski and Coworkers, *Langmuir*, **17**, 7011, 2001.
(33) V. Bergeron, PDMS Based Antifoams. In *Foams and Films*, Ed. D. Weaire and J. Banhart, MIT Verlag, Bremen, Germany, pp.41–47, 1999.
(34) S. J. Routledge, Beyond Defoaming, Antifoams on Bioprocess Productivity, *Comput. Struct. Biotechnol. J.*, **3**(4), 1–7, 2012.
(35) J. B. Winterburn and P. J. Martin, Mechanism of Ultrasound Interactions, *Asia Pac. J. Chem. Eng.*, **4**, 184–190, 2009.

(36) N. Sandor and H. N. Stein, Foam Destruction by Ultrasonics, *J. Colloid Interface Sci.*, **161**, 265–267, 1993.
(37) S. C. Sun, *Min. Eng.*, **10**, 865, 1951.
(38) A. E. Dorsey, Control of Foam during Fermentation by the Application of Ultrasonic Energy, *J. Biochem. Microbio. Technol. Eng.*, **1** (3), 289, 1959.
(39) M. D. Morey, N. S. Deshpande and M. Barigou, Destabilization by Mechanical Ultrasonic Vibrations, *J. Colloid Interface Sci.*, 1999.
(40) G. J. Freeman, A. I. Reid, C. Valdecantos Martinez, F. J. Lynch and Gallego Juarez, The Use of Ultrasonics to Suppress Foaming in Fermenters, in Proceedings of 26th European Brewery Convention (EBC) in Maastricht, Netherlands, Elsevier, pp. 405–412, May 1997.
(41) A. C. Dedhia, P. V Ambulgekar and A. B. Pandit, Static Foam Destruction: Role of Ultrasonics, *Ultrasonics*, **11**, 67–75, 2004.
(42) S. V. Komarov and Coworker, Suppression of Slag Foaming by a Sound Wave, *Ultrason. Sonochem.*, **7**, 193–199, 2000.
(43) G. Rodriguez and Coworkers, *Experimental Study of Defoaming by Air-Borne Power Ultrasonic, Int. Congress of Ultrasonics*, University of Santiago, Chile, January 2009.
(44) B. Salem and Coworkers, Propagation of Ultrasound in Aqueous Foams: Bubble Size Dependence and Resonance Effects, *Soft Matter*, **9**, 1194–202, 2012.
(45) O. Cheah and J. J. Cilliers, Foaming Behaviour of Aerosol OT Solutions at Low Concentrations Using a Continuous Plunging Jet Method, *Colloids Surf., A*, **263**, 347–352, 2005.
(46) M. Papara, X. Zabulis and T. D. Karapantsios, Container Effects on the Free Drainage of Wet Foams, *Chem. Eng. Sci.*, **64**, 1404–1415, 2009.
(47) A. F. Zuidberg, *Physics of Foam Formation on a Solid Surface in Carbonated Liquids*, PhD Thesis, Wageningen Agricultural University, Holland, 1997, ISBN 90-5485-697-1.
(48) C. A.E. Hamlett, J. D. Wallis, R. J. Pugh and D. J. Fairhurst, The Effect of Vessel Wettability on the Foamability of "Ideal" Surfactants and "Real-World" Beer Heads, *J. Am. Soc. Brew. Chem.*, **73** (3), 280–286, 2015.